

T.C.

DOKUZ EYLUL UNIVERSITY

IZMIR INTERNATIONAL BIOMEDICINE AND GENOME INSTITUTE

**ISOLATION AND CHARACTERIZATION OF
PULMONARY LUNG EPITHELIAL CELLS
FROM MICE**

İREM ŞİMŞEK

MOLECULAR BIOLOGY AND GENETICS

MASTER OF SCIENCES THESIS

IZMIR-2019

THESIS ID: DEU.IBG.MSc.2016850017

T.C.
DOKUZ EYLUL UNIVERSITY
IZMIR INTERNATIONAL BIOMEDICINE AND GENOME INSTITUTE

**ISOLATION AND CHARACTERIZATION OF
PULMONARY LUNG EPITHELIAL CELLS
FROM MICE**

MOLECULAR BIOLOGY AND GENETICS

MASTER OF SCIENCES THESIS

İREM ŞİMŞEK

Supervisor: Assoc. Prof. Ralph Leo Johan MEUWISSEN

TUBITAK 116S493

THESIS ID: DEU. IBG.MSc.2016850017

Dokuz Eylül Üniversitesi İzmir Uluslararası Biyotıp ve Genom Enstitüsü Genom
Bilimleri ve Moleküler Biyoteknoloji Anabilim Dalı,
İngilizce Moleküler Biyoloji ve Genetik Yüksek Lisans programı öğrencisi İrem
ŞİMŞEK '**Fareden Pulmoner Akciğer Epitel Hücre İzolasyonu ve
Karakterizasyonu**' konulu Yüksek Lisans tezini 09.07.2019 tarihinde başarılı
olarak tamamlamıştır.

Doç. Dr. Ralph Leo Johan MEUWISSEN
BAŞKAN

ÜYE

Doç. Dr. Duygu SAĞ WINGENDER
Dokuz Eylül Üniversitesi

ÜYE

Prof. Dr. Gülperi ÖKTEM
Ege Üniversitesi

YEDEK ÜYE

Prof. Dr. Hülya AYAR KAYALI
Dokuz Eylül Üniversitesi

YEDEK ÜYE

Prof. Dr. Serdar ÖZÇELİK
İzmir Yüksek Teknoloji Enstitüsü

Dokuz Eylul University Izmir International Biomedicine and Genome Institute
Department of Genomics and Molecular Biotechnology,
Molecular Biology and Genetics graduate program Master of Science student İrem
ŞİMŞEK has successfully completed her Master of Science thesis titled '**Isolation
and Characterization Of Pulmonary Lung Epithelial Cells From Mice**' on the
date of 09.07.2019

Assoc. Prof. Ralph Leo Johan MEUWISSEN

CHAIR

MEMBER

Assoc. Prof. Duygu SAĞ WINGENDER
Dokuz Eylul University

MEMBER

Prof. Dr. Gülperi ÖKTEM
Ege University

SUBSTITUTE MEMBER

Prof. Dr. Hülya AYAR KAYALI
Dokuz Eylul University

SUBSTITUTE MEMBER

Prof. Dr. Serdar ÖZÇELİK
Izmir Institute of Technology

TABLE OF CONTENTS

TABLE OF CONTENTS	I
LIST OF TABLES	IV
TABLE OF FIGURES	V
ABBREVIATIONS	IX
ACKNOWLEDGEMENTS	XII
ABSTRACT	1
ÖZET	2
1. INTRODUCTION AND OBJECTIVES	3
1.1 Problem Definition and Importance	3
1.2 Research Objective	4
1.3 Research Hypothesis	4
2. LITERATURE REVIEW	5
2.1 Lung Cancer	5
2.1.1 Non-small cell lung cancer	6
2.2 KRAS.....	6
2.3 Clara cells.....	11
2.4 Alveolar Type II Cells	11
2.5 Extracellular Matrix.....	13
2.6 Integrin	15
2.7 Focal Adhesion Kinase	16
2.8 Cell Immortalization	19
3. MATERIAL AND METHODS	21
3.1 Type of Research	21
3.2 Time and Place of Research.....	21
3.3 Universe and Sample of Research	21
3.4 Materials of Research	21

3.5	Variables of Research	22
3.6	Data Collection Methods	22
3.6.1	Animal Experiments	23
3.6.2	Lung Cell Isolation	23
3.6.2.1	Preparation of the Mouse Lung	24
3.6.2.2	Enzymatic Digestion of the Lung Tissue	24
	For Clara cells	24
	For Alveolar type II cells	25
3.6.2.3	Preparation of the Lung Cell Suspension	25
	For Clara cells	25
	For Alveolar type II cells	25
3.6.2.4	Antibody Staining for Flow Cytometric Cell-Sorting	26
	For Clara cells	26
	For Alveolar type II cells	27
3.6.3	Intracellular Staining For Flow Cytometry Analysis	28
3.6.4	Immunofluorescence Experiment	28
3.6.5	Immortalization of cells	29
3.6.5.1	Plasmid Preparation and Transformation	29
3.6.5.2	Plasmid DNA Isolation (Maxi Prep)	31
3.6.5.3	Preparation of PLAT-E Cells	31
3.6.5.4	Transfection	31
3.6.5.5	Viral Transduction	32
3.6.5.6	Puromycin Selection	32
3.7	Research Plan	32
3.8	Limitations of Research	34
3.9	Ethical Committee Approval	35
4.	RESULTS	36
4.1	Clara cell isolation and immunofluorescence experiment	37
4.2	Crude Lung Cell Immortalization	44
4.3	Flow Cytometry and Immunofluorescence Experiments	48
5.	DISCUSSION	52

5.1 Acquiring Lung Cells from Mouse Lung Tissue.....	52
5.2 Flow Cytometry Experiment.....	54
5.3 Immunofluorescence Experiment	55
6. CONCLUSIONS AND RECOMMENDATIONS	57
7. REFERENCES	58



LIST OF TABLES

	Page
Table 3.1: Mice types and numbers that were used in experiments are given with their dates.	21
Table 3.2: HITES medium content	22
Table 3.3: Antibody cocktail content	23



TABLE OF FIGURES

- Figure 2.1:** **A.** Normal RAS protein states. **B.** Mutated Ras signaling. Oncogenic Ras favor the binding to GTP by eliminating GAP-binding that results in the constitutively active form of RAS to exerts its oncogenic activity through different downstream signaling pathways like RAF/MEK/ERK and PI3K (13). 7
- Figure 2.2 (A)** Ad5-SPC-Cre virus represents Cre-recombinase activated SPC expressing AECII cells (yellow). K-Ras^{G12D} activity in AECII cells (green halo) causes the formation of adenoma and adenocarcinoma in the alveoli. Whereas the cells in bronchiolar part and bronchoalveolar duct junction (BADJ) remain normal. **(B)** Ad5-CC10-Cre virus target Clara cells (blue) in the bronchiolar lining and CC10/SPC dual positive cells (BASC cells) in BADJ (brown). In K-Ras^{G12D} mice, BASC cells and Clara cells trigger the formation of papillary hyperplasia at the bronchoalveolar duct junction site. Additionally, several hyperplastic cells acquire AECII cell marker, SPC expression and cause adenocarcinomas in the alveoli (5). 10
- Figure 2.3** Schematic illustration of epithelial cells along the airway tree. Localization of lung cells is represented. NEB: Neuroepithelial body, BADJ: Bronchoalveolar duct junction (28). 13
- Figure 2.4:** Schematic view of bidirectional integrin signaling. Recruitment of adaptor molecules to the β subunit of integrin triggers a conformational change in integrin to become active this is known as 'inside-out' signaling. The active form of integrin interaction to ECM, 'outside-in' signaling, further triggers downstream signaling pathways. The 'outside-in' signaling response mainly requires the involvement of FAK and subsequently Src upon their phosphorylation. Integrins exert their effects through the activation of PI₃K-AKT and RAS-MAPK. Endocytosed integrins and ECM ligands/receptor tyrosine kinases (RTKs) can further activate the 'inside-in' signaling in the cell (33). 15
- Figure 2.5:** Overview of integrated relation of integrin, receptor tyrosine kinase epidermal growth factor (EGFR), RAS, MAPK and PI₃K-Akt signaling pathways. Activation of EGFR upon its ligand binding activates growth factor receptor-bound

protein 2 (GRB2) and son of sevenless (SOS) interaction. The formation of the GRB2-SOS complex further activates RAS, downstream effector of EGFR signaling. RAS activation triggers signaling cascade involving MAPK (RAF-MEK-ERK) and PI₃K-AKT pathways. In addition to EGFR activation, integrin-ECM interaction could recruit these signaling cascades through the activation of FAK and SFKs (39). . 18

Figure 2.6: Schematic illustration of extended cellular lifespan via conditional immortalization technique. 20

Figure 3.1: pBABE SV40 puro PKB1217 plasmid map which was taken from SnapGene Viewer. 30

Figure 3.2: Illustration of initial experimental procedure. 32

Figure 3.3: Illustration of second experimental procedure. 33

Figure 3.4: Schematic view of immortalization procedure. 34

Figure 4.1 Schematic overview of isolation protocol for CCSP positive cells from mouse lung (42). 37

Figure 4.2 Sorting data of total lung cells. **A.** Crude lung cells were only incubated with secondary antibody goat anti-rabbit FITC. To discriminate dead/alive cells, cells were stained with DAPI. **B.** The whole lung cell suspension was incubated with CCSP primary antibody during an one-hour incubation; secondary antibody goat anti-rabbit FITC incubation was performed. Again to discriminate dead/alive cells, cells were treated with DAPI. After several gating processes, P3 was chosen as FITC positive population that represents CCSP⁺ cells. 38

Figure 4.3 Microscope images of cells after ACK lysis buffer treatment and before sorting **A.** 10x magnification of lung cells. **B.** 20x magnification of lung cells. ... 39

Figure 4.4 FACS ARIA III sorting result. **A.** Control cells were stained only with secondary antibody and DAPI. **B.** FITC histogram graph and FITC⁺ cell populations with percentage were given. **C.** Sample in A after 30 minutes. In histogram figure, a shift was observed in x-axis that results in a decrease of FITC⁺ population. .. 41

Figure 4.5 A. Sorted cells were put into a flask and supplied with HITES medium immediately after sorting. **B.** Cells three days after sorting. 41

Figure 4.6 FACS ARIA III sorting result. **A.** Control cells were stained with Alexa 647 **B.** Anti-CCSP labeled Alexa 647⁺ cell population with percentage was given. **C.** .

Control cells were stained with FITC **D.** Anti-CCSP labeled FITC⁺ cell population with percentage was given. 42

Figure 4.7 Immunofluorescence experiment images of labeled CCSP cells. **A.** Alexa Fluor 647 staining of CCSP labeled cells. After counting, unsorted cells were separated and plated onto coverslips for IF experiment. Images were taken two days after isolation in 40X magnification. **B.** Alexa Fluor 647 staining of sorted CCSP⁺ cells. CCSP⁺ cells were seeded onto coverslips for IF staining. Images were taken one day after sorting in 40X magnification. 43

Figure 4.8: Determination of puromycin concentration for selection and control groups. Images were taken under 10x magnification. **A.** Control lung cells without viral transduction and without puromycin application. **B.** Untransduced lung cells with 250ng/ml puromycin application. **C.** Untransduced lung cells with 500ng/ml puromycin application. **D.** Polybrene control in untransduced and non-puromycin applied cells. **E.** Transduced lung cells with 250ng/ml puromycin application. **F.** Virus transfected lung cells with 500ng/ml puromycin application. 45

Figure 4.9: Determination of puromycin concentration for selection and control groups. Images were taken under 10x magnification. **A.** Control lung cells without viral transduction and without puromycin application. **B.** Untransduced lung cells with 500ng/ml puromycin application. **C.** Untransduced lung cells with 1000ng/ml puromycin application. **D.** Polybrene control in untransduced and non-puromycin applied cells. **E.** Transduced lung cells with 500ng/ml puromycin application. **F.** Virus transfected lung cells with 1000ng/ml. 46

Figure 4.10: Determination of puromycin concentration for selection and control groups. Images were taken under 10x magnification. **A.** Control lung cells without viral transduction and without puromycin application. **B.** Untransduced lung cells with 2000ng/ml puromycin application. **C.** Untransduced lung cells with 3000ng/ml puromycin application. **D.** Transduced lung cells with 200ng/ml puromycin application. **E.** Virus transfected lung cells with 3000ng/ml. 47

Figure 4.11: Flow cytometry analysis data of transduced cells **A.** Control cells were stained with Alexa Fluor 647. **B.** Immortalized lung cells were fixed and treated

with anti-CCSP antibody and then stained with Alexa Fluor 647 for further analysis.
..... 48

Figure 4.12: FACS ARIA III sorting result. **A.** Cells were stained with with Alexa Fluor 647 secondary antibody. DAPI staining was performed to discriminate dead/alive cells. **B.** CCSP antibody treated cells were stained with Alexa Fluor 647 secondary antibody. DAPI staining was performed to discriminate dead/alive cells. After several gating processes, P3 was chosen as CCSP labeled Alexa Fluor 647⁺ cell population. 49

Figure 4.13: Immunofluorescence images CCSP⁺ cells. **A.** Alexa Fluor 647 staining of unsorted immortalized CCSP labeled lung cells. Images were taken in 20X magnification. **B.** Alexa Fluor 647 staining of sorted immortalized CCSP labeled lung cells. Sorted CCSP⁺ cells in Figure 4.12 were seeded onto coverslips for IF staining. Images were taken in 20X magnification. **C.** 40x magnified version of cells in B. 50

Figure 4.14: Flow cytometry data of proSPC labeled cells. **A.** Control cells were stained with Alexa Fluor 647. **B.** Immortalized lung cells were fixed and intracellular stained. Anti-proSPC antibody was used as primary antibody and then cells were stained with Alexa Fluor 647. 51

Figure 5.1: Immunofluorescence staining of CCSP labeled cells in Wang, Keefe, Jensen-Taubman, Yang, Yan and Linnoila (42) reference paper. They found that CCSP⁺ sorted cells were also positive for CCSP IF with higher percentage compared to unsorted cells. 56

ABBREVIATIONS

AAH	Adenomatous hyperplasia
ACK	Ammonium-Chloride-Potassium
AECII	Alveolar type II cell
AKT	Protein kinase B
ALK	Anaplastic lymphoma kinase
APC	Allophycocyanin
BADJ	Bronchoalveolar duct junction
BASC	Bronchioalveolar stem cell
BRAF	B-Raf proto-oncogene
C57BL/6	C57 black 6
CC10	Club cell protein 10
CC16	Club cell protein 16
CCSP	Clara cell secretory protein (4',6-Diamidino-2-Phenylindole, Dihydrochloride)
DAPI	
DH5 α	5-alpha Competent E. coli
DMEM	Dulbecco's Modified Eagle's Medium
ECM	Extracellular Matrix
EGFR	Epidermal growth factor receptor
ERK1/2	Extracellular signal-regulated kinases
FACS	Fluorescence-activated cell sorting
FAK	Focal adhesion kinase
FBS	Fetal Bovine Serum
FITC	Fluorescein isothiocyanate
GAP	GTPase-activating proteins
GDP	Guanosine diphosphate
GEF	Guanine nucleotide exchange factors
GRB2	Growth factor receptor-bound protein 2

GTP	Guanosine triphosphate
GTPase	Guanosine triphosphatase enzyme
HEPES	(4-(2-hydroxyethyl)-1-piperazineethanesulfonic acid)
HITES	Hydrocortisone, insulin, transferrin, estrogen, and selenium
HRAS	Harvey rat sarcoma viral oncogene homolog
IBG-Izmir	Izmir International Biomedicine and Genome Institute
IF	Immunofluorescence
ITS	Insulin transferrin selenium
IVC	Inferior vena cava
KRAS	Kirsten rat sarcoma viral oncogene homolog
LB	Luria Broth
LT	Large T
MAPK	Mitogen-activated protein kinase
MEF	Mouse embryonal fibroblast
MEK1/2	Mitogen-activated protein kinase kinases
NRAS	Neuroblastoma rat sarcoma viral oncogene homolog
NSCLC	Non-small cell lung cancer
p53	Tumor suppressor p53
PBS	Phosphate buffered saline
PE	Phycoerythrin
Pen-Strep	Penicillin-Streptomycin
PH	Pleckstrin homology
PI3K	Phosphoinositide 3 kinase
PIP2	Phosphatidylinositol (4, 5)-biphosphate
PIP3	Phosphatidylinositol (3,4,5)-triphosphate
PLAT-E	Platinum-E

pRB	Retinoblastoma
proSP-C	Prosurfactant Protein C
RAF	Rapidly accelerated fibrosarcoma
RAS	Rat sarcoma
RTK	Receptor tyrosine kinase
SCGB	Secretoglobulin
SCLC	Small cell lung cancer
SFK	Src-family kinase
SOS	Son of sevenless
SPC	Surfactant protein C
SV40	Simian virus 40
TME	Tumor microenvironment
WT	Wild-type
α	Alpha
β	Beta

ACKNOWLEDGEMENTS

I would like to express my special thanks to my advisor Assoc. Prof. Ralph Leo Johan Meuwissen for his valuable support, extensive knowledge and most importantly for his faith in me during my research. He gave me the opportunity to work in his lab and provided me with encouragement and patience throughout my master study.

I am also grateful to my postdocs Tuğşen Aydemir and Hadi Rouhrazi for their support and assistance. Especially Tuğşen Aydemir who also assigned to this project, extended a great amount of assistance. Without her support, help, encouragement, tolerance and most importantly her friendship this process would be much more difficult.

Furthermore, I also had great pleasure of working with our previous member of Meuwissen lab Merve Torun. I am also grateful to my previous postdoc Aslı Sade for her support and guidance. Moreover, this process would not be possible without the support and friendship of my friends in IBG.

I would like to extend my gratitude to all members of IBG Vivarium core facility, IBG Flow Cytometry core facility and IBG Imaging core facility for their assistance and effort.

I would also like to thank to TUBITAK 2211 Domestic Graduate Scholarship Program to support me.

I would also like to thank Ali Kemal Baş for his belief, friendship, and endless love. He was there for me whenever I was in need.

Lastly and most importantly, I would like to thank my dearest family members for their endless support and faith in me. Without their presence, none of this would be possible.

ISOLATION AND CHARACTERIZATION OF PULMONARY LUNG EPITHELIAL CELLS FROM MICE

İrem ŞİMŞEK

Izmir International Biomedicine and Genome Institute, Dokuz Eylül University

irem.simsek@msfr.ibg.edu.tr

ABSTRACT

Non-small cell lung cancer (NSCLC) is the most prevalent lung cancer type. It has become a topic of numerous research to enlighten its ontogeny and molecular pathogenesis during the decade. However, an efficient targeted therapy has still not emerged. Thus, there is a need for more effective therapies against NSCLC.

NSCLC mainly originates from Clara cells and alveolar type II cells thus due to their vital role in NSCLC; in this project, it is aimed to isolate these cell types from mice and upon their isolation they will be immortalized. In this way, we will have created our own cell lines for our later studies other than this project. The main reason for this is to optimize our procedure and try to make straight-forward protocol.

During the research, Clara cells are successfully isolated and immortalized, and alveolar type II cells are about to be isolated. Although some complications, we have successfully optimized our protocols and it is possible to apply the methods that are covered in this project without any hesitation and time loss.

Key Words: Non-small cell lung cancer, Clara cells, Alveolar type II cells

FAREDEN PULMONER AKCİĞER EPİTEL HÜCRE İZOLASYONU VE KARAKTERİZASYONU

İrem ŞİMŞEK

İzmir Uluslararası Biyotıp ve Genom Enstitüsü, Dokuz Eylül Üniversitesi

irem.simsek@msfr.ibg.edu.tr

ÖZET

Küçük hücreli dışı akciğer kanseri (KHDAK) en sık görülen akciğer kanseri türüdür. Ontojenitesini ve moleküler patojenezini aydınlatmak amacıyla on yıldır sayısız araştırmaya konu olmuştur fakat hala etkili bir hedefe yönelik terapi ortaya çıkmamıştır. Bu nedenle KHDAK'ne karşı etkili tedavilere ihtiyaç vardır.

KHDAK, esas olarak Clara hücrelerinden ve alveoler tip II hücrelerinden başlar, KHDAK'deki önemli rolleri nedeniyle; bu projede, bu hücre tiplerinin farelerden izole edilmesi ve izolasyonları üzerine ölümsüzleşmeleri amaçlanmaktadır. Bu şekilde, bu proje dışındaki başka çalışmalarımız için kendi hücre hatlarımızı yaratacağız. Bu projenin esas amacı protokollerimizi optimize etmek ve protokolü rahatlıkla uygulanabilir hale getirmektir.

Araştırma sırasında Clara hücreleri başarılı bir şekilde izole edilmiş ve ölümsüzleştirilmiştir. Alveolar tip II hücreleri de izole edilmek üzeredir Bazı komplikasyonlarla karşı karşıya kalınmasına rağmen, protokollerimizi başarıyla optimize ettik ve bu projede yer alan yöntemleri tereddüt etmeden ve zaman kaybetmeden uygulamak mümkündür.

Anahtar Kelimeler: Küçük hücreli dışı akciğer kanseri, Clara hücreleri, Alveolar tip II hücreleri

1. INTRODUCTION AND OBJECTIVES

1.1 Problem Definition and Importance

Lung cancer is the most common and by far the most lethal cancer type in the world. Lung cancer has become the leading cause of cancer death since worldwide annual death rate is more than 1,8 million (1). NSCLC is one of the major histopathological groups of lung cancer and the incidence rate of NSCLC is approximately 85% among all lung cancers (2). NSCLCs can be subcategorized into adenocarcinoma (60%), squamous cell carcinoma (30%), and large cell carcinoma (10%). Survival rate is considerably high in early stage NSCLC. Patients with metastatic NSCLC, however, show a sharp decrease in survival rates and generally require additional chemo- or radiotherapy based (combinatorial) treatments. Therefore, advanced stage patients no longer benefit from surgical operations alone as early stage patients do (3). Recent advanced surgical techniques have somewhat improved survival rates. Main problem still lies with advanced NSCLC need for non-surgical therapies whereby novel targeted therapies are often still may not sufficient for proper treatment. The latter effect is largely due to the intrinsic or acquired resistance capacity of NSCLC, which causes a high risk of recurrence (4).

NSCLC contains a vast amount of dominant 'driver' mutations that cause lung cancer initiation and progression (2). One of these driver mutations has been found to affect Kirsten rat sarcoma viral oncogene homolog (KRAS) and has been observed in around 20-30% of all NSCLC (5).

KRAS regulates several cellular signaling pathways of which especially RAF/MEK/ERK and PI3K/AKT/mTOR are the most active ones, whereby and these pathways are main targets through which dominant-active mutant KRAS exerts its oncogenic activity (6). Mutated Kras is therefore an attractive target for any tumor intervention therapy but up-to-date results of all therapeutic applications remain poor. To investigate and understand the oncogenic activity of KRAS, Cre/lox technology was used to create a somatic RasF mouse model whereby mutant KRAS^{G12D} lesions are

generated into lung epithelial cells leading to the development of NSCLC (7, 8). With the advancement of these models, it is possible to mimic the NSCLC tumorigenesis.

RasF mouse model also enlighten the cell origin of KRAS^{G12D} mediated NSCLC. By using this model, it has been shown that alveolar type II cells and Clara cells are mainly responsible for the initiation of KRAS^{G12D} triggered NSCLC.

That is why we mainly focus on these cell types and in this project our aim is to isolate these cells and after their isolation we are planning to immortalize these cells to generate our cell lines to use them for future experiments and projects. This study has a characteristic of a sub-project and the work that is covered in this thesis create the infrastructure of the main project. Optimizing each experiment in this project and creating our own cell lines has a vital role for further studies.

1.2 Research Objective

In this project, in order to obtain Clara and Alveolar type II epithelial cells we will isolate these cells from mice and then we will transform these cells into immortalized cells by inhibiting senescence activity, to create our own cell lines rather than commercial ones. The reason for constructing our cell lines is compare to commercial cell lines these transformed cells show close resemblance to human cells. If we achieve our aim, it will be possible to use these methods for mutant mice other than wild types to enlighten the molecular mechanism of KRAS^{G12D}.

1.3 Research Hypothesis

Isolation and immortalization of pulmonary lung epithelial cells will provide us the characterization of these cell types and created cell lines will further will represent great tools to study for KRAS^{G12D} triggered NSCLC.

2. LITERATURE REVIEW

2.1 Lung Cancer

Cancer is a complex disease and according to GLOBOCAN updates in 2018, 18.1 million new cancer cases and 9.6 million cancer-related deaths were projected worldwide (1).

Cancer is a disease of uncontrolled proliferation of dedifferentiated cells.. It is the result of continuous molecular changes that take place in cancer cells, among which there are augmented intrinsic survival activities causing cells to alter their regular properties (9). Therefore, cancer can be characterized as a reduction or loss of normal cellular regulation and/or developmental mechanism because of (epi)genetic alterations. Alterations in proto-oncogenes and tumor-suppressor genes have a crucial role in cancer stimulation. These alterations are so-called mutations and commonly result in the rapid growth of cells (10).

Lung cancer is the most frequently diagnosed cancer type with the highest death rate. It is one of the most common cancer types with 2.09 million new cases and 1.76 cancer-related deaths in both men and women (1).

Lung cancer has two major subtypes with different histological characteristics known as NSCLC and small cell lung cancer (SCLC). NSCLC is by far the most common type since it constitutes about 85% of all lung cancers (11). NSCLC can be divided into several subgroups in itself according to their initiation ways. Adenocarcinoma, squamous cell carcinoma, and large cell carcinoma are the most prevalent types of NSCLC respectively.

Lung cancer, especially NSCLC is mainly associated with smoking and it is the leading cause of squamous-cell carcinoma and large cell carcinoma. Smoking also affects adenocarcinoma formation. However, adenocarcinoma can also occur in nonsmokers. Although smoking is the most prominent cause of lung cancer, industrial development based environmental pollution accelerate the mortality risk of lung cancer (2).

Other than environmental factors, as in all cancers, hereditary factors can also increase the incidence of lung cancer. People with a family history are more prone to lung cancer due to genetic heritage (2).

2.1.1 Non-small cell lung cancer

NSCLC stages are determining in how far the tumor has developed by growing and spreading. Tumor stages are therefore essential in assessing prognosis and therapy choices. Early stages of NSCLC are often treatable with surgical operations. Nowadays, thanks to technological advancements, respectable tumor lesions can be removed easily without making large incisions in the early stages of NSCLC. Following surgical operations, patients are given adjuvant therapy to reduce the recurrence risk of cancer (2).

However, it is not always possible to diagnose NSCLC during early onset. Most of the patients are diagnosed at late, metastatic stage IV. For such patients, combinatorial chemotherapy is generally the first option to reduce the disease-related effects and to increase the chance of patient survival. However, the application of highly toxic drugs may not be beneficial for every patient due to potential adverse effects of drugs. Radiotherapy is another option for patients who cannot benefit from surgical operations or chemotherapy (2).

Developments in molecular cancer genetics and genome analysis revealed several 'driver' mutations that could become targets for tumor intervention therapy. Epidermal growth factor receptor (EGFR), anaplastic lymphoma kinase (ALK), KRAS and B-Raf proto-oncogene (BRAF) are several of such candidates in NSCLC targeted therapies (2).

2.2 KRAS

Rat sarcoma (RAS) protein is a member of small guanosine triphosphatase enzyme (GTPases) and known as a driver oncogene in different cancers. RAS proteins take parts in vital developmental processes like cell growth, proliferation, and survival.

RAS has two conformational forms; one is guanosine diphosphate (GDP) bound and, the other one is guanosine triphosphate (GTP) bound. GTP bound form of RAS is the active form, "on state" of RAS (6, 12). Transitions of these states are regulated via GTPase-activating proteins (GAP) and guanine nucleotide exchange factors (GEF). Hydrolysis of GTP to GDP is catalyzed by GAP and the reverse event is regulated by GEF (Figure 2.1) (13). Mutated Ras acts as an oncogene by constitutively binding GTP thus, disrupting the molecular switch and GAP no longer can bind to RAS that leads to constitutively active RAS, which favors continuous activation of the RAS-dependent downstream oncogenic signaling (Figure 2.1) (12, 14). Activated RAS has various effectors, which in turn triggers different signaling pathways. Most well-known and characterized ones are mitogen-activated protein kinase (MAPK) and phosphoinositide 3 kinase (PI3K) signaling pathways (Figure 2.1) (6).

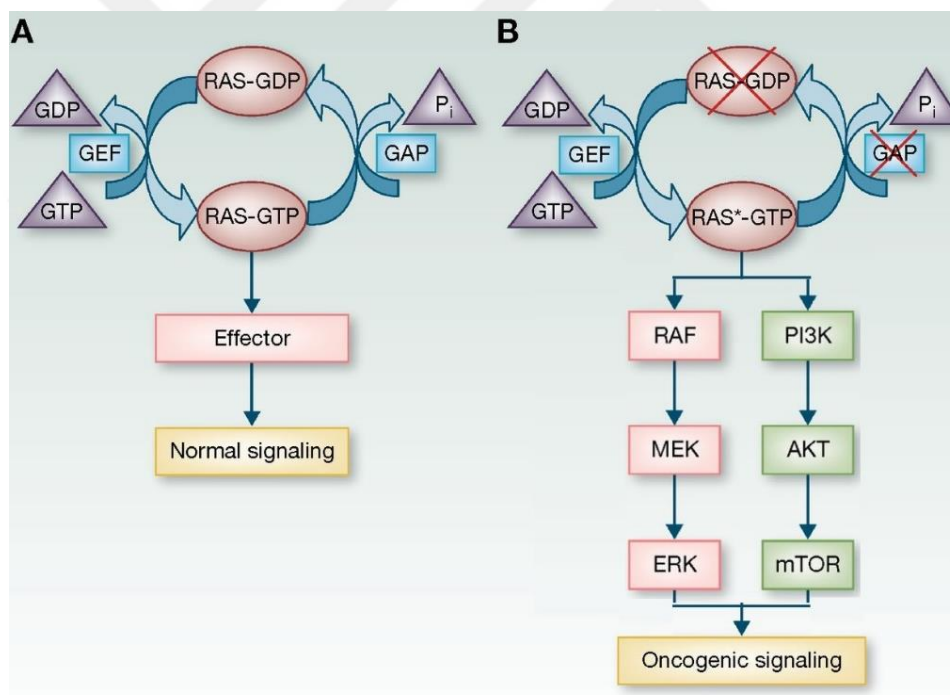


Figure 2.1: **A.** Normal RAS protein states. **B.** Mutated Ras signaling. Oncogenic Ras favor the binding to GTP by eliminating GAP-binding that results in the constitutively active form of RAS to exerts its oncogenic activity through different downstream signaling pathways like RAF/MEK/ERK and PI3K (13).

A serine/threonine kinase **R**apidly **a**ccelerated **f**ibrosarcoma (RAF) is a key protein in the MAPK pathway, its binding to GTP-RAS effector region phosphorylates mitogen-activated protein kinase kinases (MEK1/2) which further activates extracellular signal-regulated kinases (ERK1/2). This pathway is highly associated with cell proliferation and differentiation (15).

PI3K pathway has an important role in cell growth, proliferation, and survival. Active PI3K has a role in the conversion of phosphatidylinositol (4, 5)-biphosphate (PIP₂) into phosphatidylinositol (3,4,5)-triphosphate (PIP₃). PIP₃ has high affinity to pleckstrin homology (PH) domain of protein kinase B (Akt) kinase, upon binding of PIP₃ to Akt, a phosphorylation cascade is triggered to regulate cell growth and cell survival (16).

Besides KRAS there are two other RAS proteins which are Harvey rat sarcoma viral oncogene homolog (HRAS) and Neuroblastoma rat sarcoma viral oncogene homolog (NRAS) and all three RAS proteins are highly conserved among species (6). Their oncogenic mutation rates are different and KRAS has the highest incidence rate with 85%, which is followed by NRAS with approximately 15% whereas HRAS is responsible for less than 1% of all mutations found in human cancers. KRAS mutations are frequently detected in pancreatic, lung and colon cancers.

KRAS is responsible for approximately 20% of lung cancers. It has the highest rate of mutations in NSCLC whereby activation of KRAS is the main oncogenic driver with occurrence in almost 30% of all NSCLC cases (12). Among the various mutations in KRAS codons, the most prominent ones are in codons 12, 13 and 61 of the G domain. The most frequent variants are G12C, G12V, and G12D (12).

Many strategies have been developed in order to target oncogenic RAS, including direct inhibition of RAS, development of small molecules, blocking its activity by targeting downstream signaling pathways. These challenging approaches to inactivate oncogenic RAS activity are not very successful so far and this is mainly due to certain aspects. GTP binding affinity for (mutated) RAS is extremely high and great quantities of GTP in cells make direct inhibition of RAS difficult. Developments still take place to restore GTPase hydrolysis however; this method is also compelling due to structural obstacles. Although direct inhibition of RAS is challenging, it is still promising

because several small molecules are under clinical trial. Other current therapeutic approaches against RAS target oncogenic activity of its downstream effectors. MAPK and PI3K pathways have drawn attention. The complexity of oncogenic RAS-driven signaling however, makes finding an effective therapeutic target difficult. Several synthetic lethal screens and drug development processes, gained a better understanding of RAS driven oncogenic signaling but at the same time, mutated RAS has preserved its untreatable characteristics (17, 18).

In order to address alternative pathways that interact with mutated RAS functions during lung tumorigenesis, we decide to make use of KRAS dependent somatic mouse models of lung cancer. With the help of these mouse models, it is possible to get an idea about tumor formation and progression also, about its natural tumor microenvironment (TME). Since the use of classical transgenic or knockout mice has some limitations in the progression of sporadic cancer, the need for new models has emerged. With the help of Cre/loxP technology, conditionally activation of oncogenes or inhibitions of tumor suppressor genes lead to the the onset of of sporadic cancer with a close resemblance to human cancer (19).

Cre/Lox system is used to turn on oncogenic Kras activity by the insertion of Lox-Stop-Lox sequence in between the transgene promoter and Kras G12D oncogene (LSL-Kras^{G12D}). Introducing Cre recombinase into the system, via adeno-Cre virus into the lung, results in the excision of Stop element which in turns activates Kras (20). Floxed mouse models are generated with the Cre/Lox system. Kras^{G12D} mice model is a great tool to study somatic lung cancer since it mimics gradual development as seen in human lung cancer. It is possible to observe the progression of lung cancer from adenomatous hyperplasia (AAH) to adenocarcinoma (8).

Kras^{G12D} mouse models have made great contributions to the determination of the cell origin of lung adenocarcinoma. Different experiments and methodologies have revealed that separate cancer initiating cells are present such as Clara cells (Club cells), Alveolar type II cell (AECII) and bronchioalveolar stem cells (BASCs, dual positive club cell protein 10 (CC10), and surfactant protein-C (SPC) cells. Developmental, environmental and genetic factors cause the cell differentiation to initiate cancer progression (21). Kras^{G12D} induced tumor progression triggers Clara cell differentiation,

and in $Kras^{G12D}$ mouse models, Clara cells transdifferentiate into Alveolar type II cells. Alveolar type II cells and Clara cells have counted as major proliferative cells in $Kras^{G12D}$ mouse models (Figure 2.2) (5).

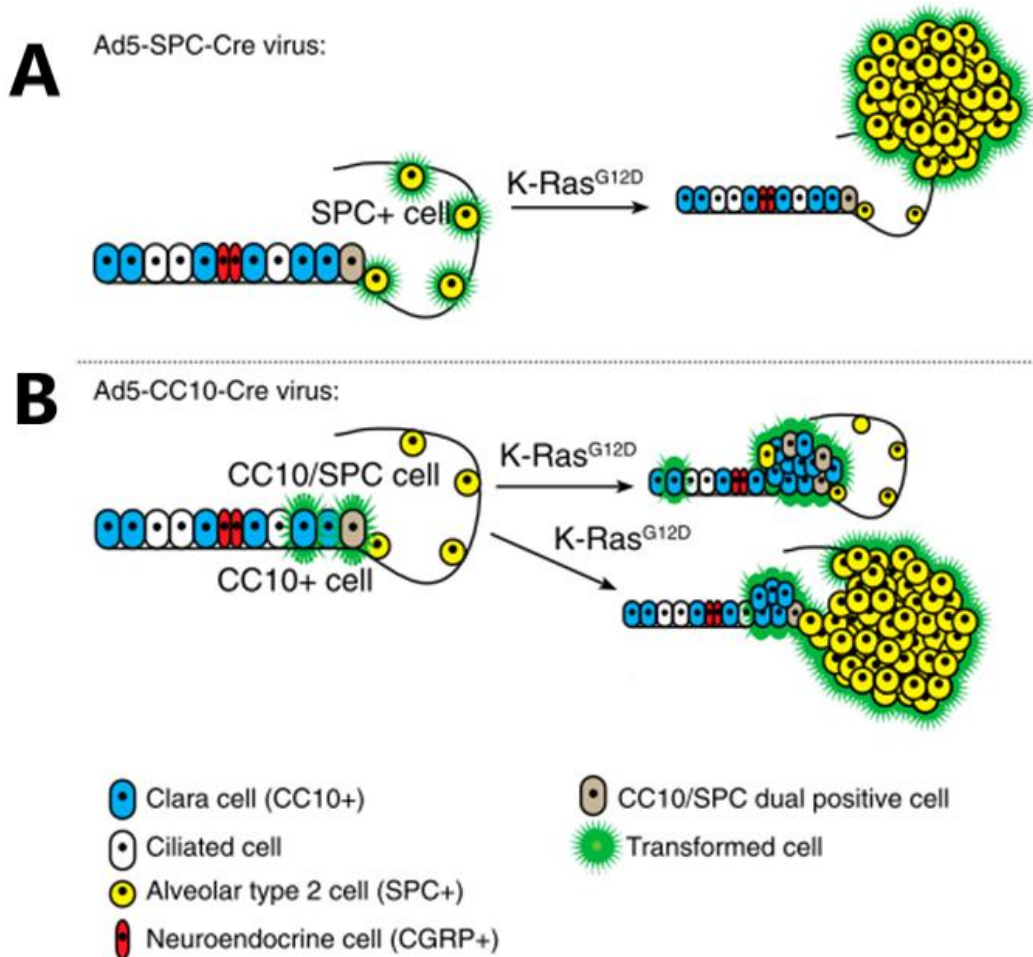


Figure 2.2 (A) Ad5-SPC-Cre virus represents Cre-recombinase activated SPC expressing AECII cells (yellow). $K-Ras^{G12D}$ activity in AECII cells (green halo) causes the formation of adenoma and adenocarcinoma in the alveoli. Whereas the cells in bronchiolar part and bronchoalveolar duct junction (BADJ) remain normal. **(B)** Ad5-CC10-Cre virus target Clara cells (blue) in the bronchiolar lining and CC10/SPC dual positive cells (BASC cells) in BADJ (brown). In $K-Ras^{G12D}$ mice, BASC cells and Clara cells trigger the formation of papillary hyperplasia at the bronchoalveolar duct junction site. Additionally, several hyperplastic cells acquire AECII cell marker, SPC expression and cause adenocarcinomas in the alveoli (5).

2.3 Clara cells

The non-ciliated bronchiolar epithelial cells, Clara cells, or Club cells are dome-shaped non-ciliated secretory cells. They are abundant in rough and smooth endoplasmic reticulum and mitochondria. In human lungs, Clara cells establish 9% of airway epithelial cells. Around 11% reside in terminal airways and constitute 15% of proliferating cells in this part, in addition, around 22% reside in respiratory bronchioles and herein they constitute 44% of all proliferating cells (Figure 2.3) (22). In literature, Clara cell protein is mentioned under different names such as uteroglobin, clara cell secretory protein (CCSP), club cell protein 16 (CC16), CC10, secretoglobin (SCGB), human protein 1 and urine protein 1. Club cells have a function as progenitor cells for themselves and for ciliated cells in small airways. Clara cells also play a role in the protection of lungs from toxic compounds that are introduced into airways during inhalation. They secrete different biological substances to regulate the inflammatory response in the damage scenario. As mentioned before, under $Kras^{G12D}$ mutation induction, they may trigger neoplasia. Due to these reasons, Clara cells are counted as protective regulatory cells in the lungs (23).

Having a progenitor capability, Clara cells are responsible for the reconstitution of damaged parts of airways. In order to repair these damages parts during injury they need to undergo certain series of events proliferation, cell spreading and eventually migration to the injured parts of airways. Clara cells are capable to sense the change in matrix components to generate response in turn (24).

2.4 Alveolar Type II Cells

AECIIs are cuboidal-shaped epithelial cells, located in the alveolar epithelium (alveoli) of lungs and establish 15% of all epithelial cells in peripheral airways (Figure 2.3). AECII cells have roles in the expression of surfactant proteins. Although type II cells do not occupy a significant place in the alveolar surface, roughly 5% of the surface area, they play fundamental roles in alveoli. AECIIs are responsible for the production and the secretion of surfactant proteins to recruit gas exchange by reducing surface

tension. Surfactants are lipoproteins and they are responsible for the maintenance of alveolar size also, they ensure the dryness of alveoli (25).

AECIIs serve as a protector in alveoli since they play a significant role in the repair process. Alveolar epithelial cells arise from type II cells and in order to restore the damaged parts of epithelium they dedifferentiate, proliferate, migrate to damaged part of alveoli to reconstitute the injured epithelial cells and when the need arises transdifferentiate into other alveolar cells like type I cells and (26, 27). Moreover, these cells are in charge of innate immunity regulation. Normally, type II cells secrete numerous anti-inflammatory, antimicrobial materials and immunoglobulins however, during infection, AECIIs and other alveolar epithelial cells augment the secretion. In addition to this, they secrete chemokines and cytokines. They maintain alveolar homeostasis by assigned as transepithelial sodium and fluid conveyance to maintain homeostasis by doing so alveolus has kept clear and fluid-free (27).

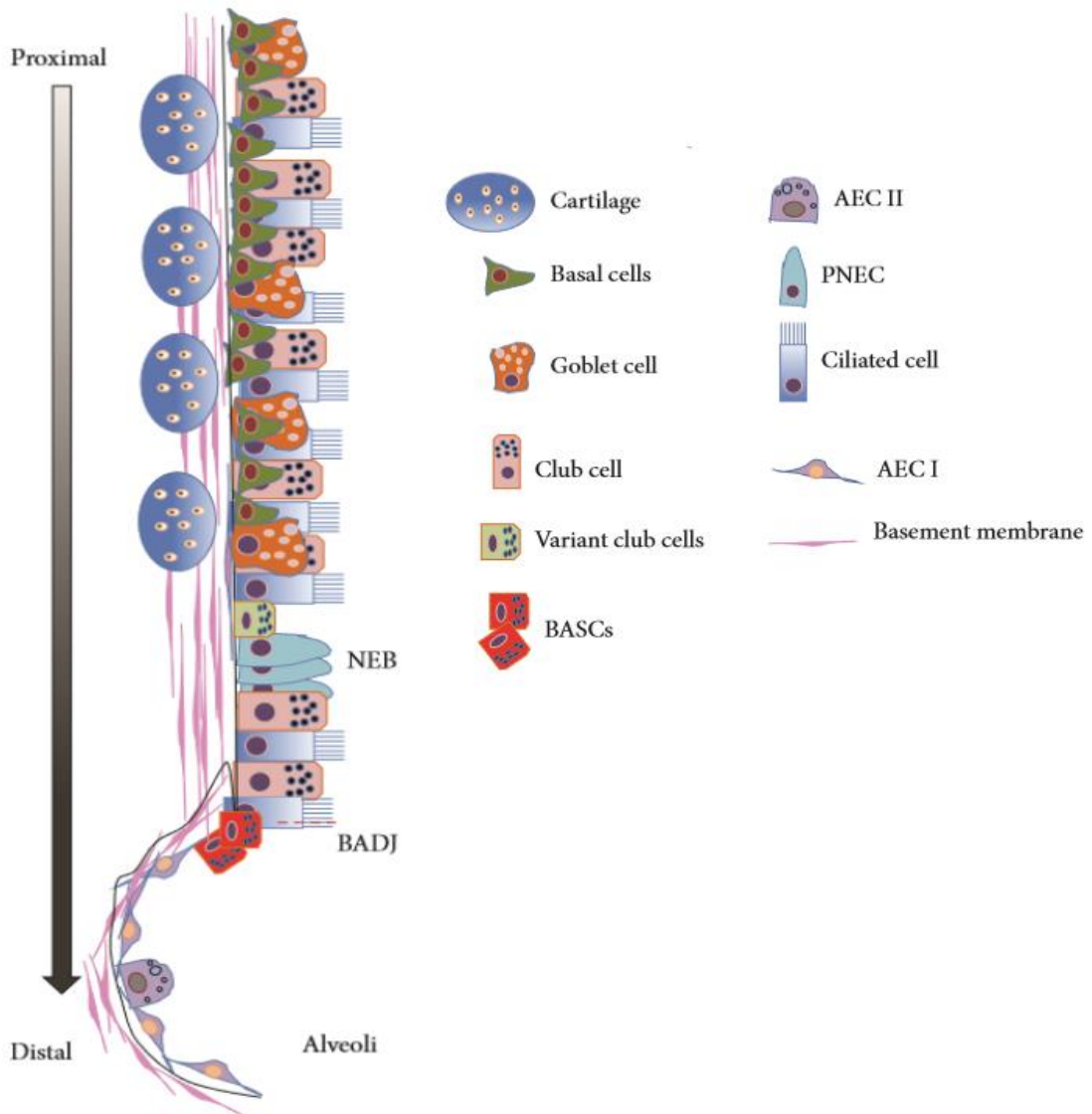


Figure 2.3 Schematic illustration of epithelial cells along the airway tree. Localization of lung cells is represented. NEB: Neuroepithelial body, BADJ: Bronchoalveolar duct junction (28).

2.5 Extracellular Matrix

Hallmarks of cancer have been investigated for decades to define many characteristics of cancer. How tumor cells affect their environment to favor its growth by influencing and interacting with surrounding normal cells, still unknown. ECM is a dynamic three-dimensional network of complex macromolecules that are secreted from neighboring cells to support cellular activity. This dynamic structure of ECM is the result

of continuous remodeling mechanism of ECM that is coordinated by ECM-modifying cells. The balance between structural formation and degradation of ECM is the key factor in the determination of cell properties (29).

The essential activity of ECM is to provide a scaffold for surrounding cells while doing this, it also presents a stiff and flexible environment, which is necessary for biochemical and biomechanical properties of cells. Furthermore, ECM stimulates cell migration to different destinations during the cellular organization and tissue remodeling. This stimulation is triggered by ECM composition concentration density. Cells can sense their migration path according to regions with different ECM concentration (29).

Loss of aforementioned compositional ECM balance results in dysregulation of ECM homeostasis. Such regulations may also cause changes in normal cellular behaviors, as in the case of cancer cell formation. This kind of ECM organizations and alterations establish tissue-specific microenvironment, influencing cancer cell formation and progression. Proliferating tumor cells recruit resident cells and alter the surrounding ECM to constitute tumor microenvironment. Alterations in ECM composition and recruitment of tumor cells cause excess protein secretion of cells that provide tumor cell to exert its effect for tumor progression. Therefore, ECM is vital for TME and accordingly, for tumor cells (29).

Other than tumor formation, the change in ECM composition is a response due to the extreme need of cells during injury. As mentioned before, Clara cells and AECII cells are responsible for the repairment of injured epithelial cells to do so they can benefit from the change of the ECM composition to respond the need of recovery and reconstitution of damaged area. Injury triggered matrix component change affects behavior of these cells. Injured epithelial cells were replenished by their migration. During this stage both Clara cells and AECIIs are directed via integrins which are the major interaction sites for cells (24).

2.6 Integrin

Integrins are heterodimers and composed of two subunits, alpha (α) and beta (β) subunits. Integrin family has 24 different members arise from dimerization of eight β and 18 α subunits. Ligand binding to integrin leads to a conformational change in its' subunits which triggers the signal transduction and cellular response (30). Integrin family has a vital role in cell adhesion to ECM, through the interaction with ECM, they can regulate cellular events; this kind of response is known as "outside-in signaling" (Figure 2.4). Integrins can also regulate their binding to other integrins or extracellular proteins via cytoplasmic interactions, which is known as "inside-out signaling" (Figure 2.4). By this means, the integrin family has a role as mechano-receptor and force-transmitter in the communication among the cells and their microenvironment (31, 32).

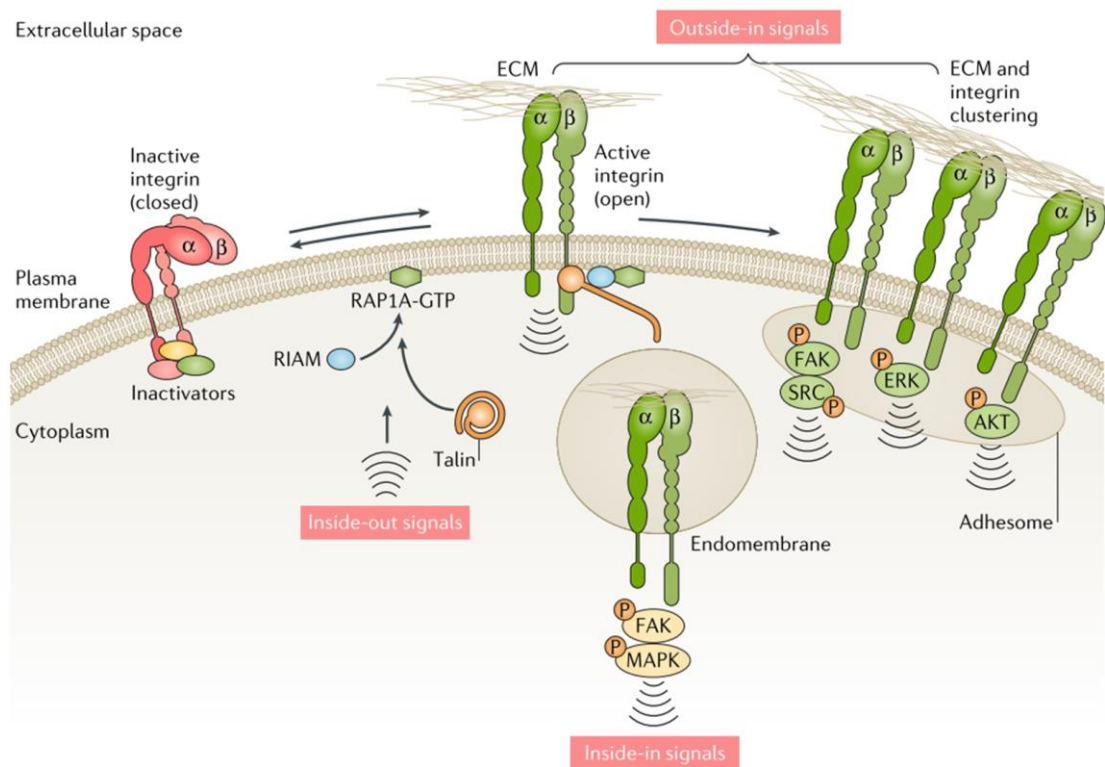


Figure 2.4: Schematic view of bidirectional integrin signaling. Recruitment of adaptor molecules to the β subunit of integrin triggers a conformational change in integrin to become active this is known as 'inside-out' signaling. The active form of integrin

interaction to ECM, 'outside-in' signaling, further triggers downstream signaling pathways. The 'outside-in' signaling response mainly requires the involvement of FAK and subsequently Src upon their phosphorylation. Integrins exert their effects through the activation of PI₃K-AKT and RAS-MAPK. Endocytosed integrins and ECM ligands/receptor tyrosine kinases (RTKs) can further activate the 'inside-in' signaling in the cell (33).

Tumor cells cause the exploitation of integrin-mediated signaling to promote tumor progression and survival. Moreover, by doing so they can restore the host microenvironment that is favorable for tumor growth and invasiveness (32). Integrin involvement in cancer development has been observed in all phases of cancer progression from the initiation to metastatic spread of cancer cells. During tumor progression, expression of integrins increases which in turn increases the 'outside-in' signaling. Upregulated signaling results in abundant ECM constituents' secretion that causes abnormal activity of ECM remodeling mechanism.

ECM composition alteration is the decision mechanism for cells to respond to the surrounding cells' needs. Cancer cells change the composition of the matrix to establish their favorable microenvironment however, cells also use this altered composition to reconstitute the repaired areas, during this stage integrin involvement is essential. Integrin activity and guidance is important during metastasis either for normal cells or tumor cells.

Integrins do not have kinase activities thus; they are in need of additional molecules to exert their signals. In this case, they are achieving signal transduction through Src-family kinases (SFKs) and FAKs (Figure 2.4).

2.7 Focal Adhesion Kinase

FAK protein is a well-known mediator of integrin signaling. ECM triggered active integrin interaction with FAK triggers phosphorylation of FAK to transfer the signal to the downstream proteins for biological responses. Phosphorylation event takes place at Y397T, which results in the binding site for the SH2 domain of Src. Src binding leads

additional phosphorylation events on FAK kinase domain to allow binding of several adaptor molecules which links integrin with Rac1 GTPase or MAPKs (31).

FAK kinase activity can also be triggered via pH and ECM tension fluctuations, which is important function for cancer progression. FAK plays a crucial role as an intermediary protein in different signaling pathways during cancer growth and metastasis. Tumor cells are in need of FAK activity in order to proliferate and metastasize (34). FAK is found to be active and overexpressed in several solid cancers, especially in NSCLC upregulated FAK has been observed (35).

As mentioned before, metastatic tumor cells require integrin activity to invade adjacent stromal cells and ECM. To achieve this, they need FAK recruitment for the activation of β integrins. Moreover, to disrupt focal adhesion proteins activity and ECM motion FAK recruitment is necessary. Thus, FAK promotion is essential for tumor spread and invasiveness (34).

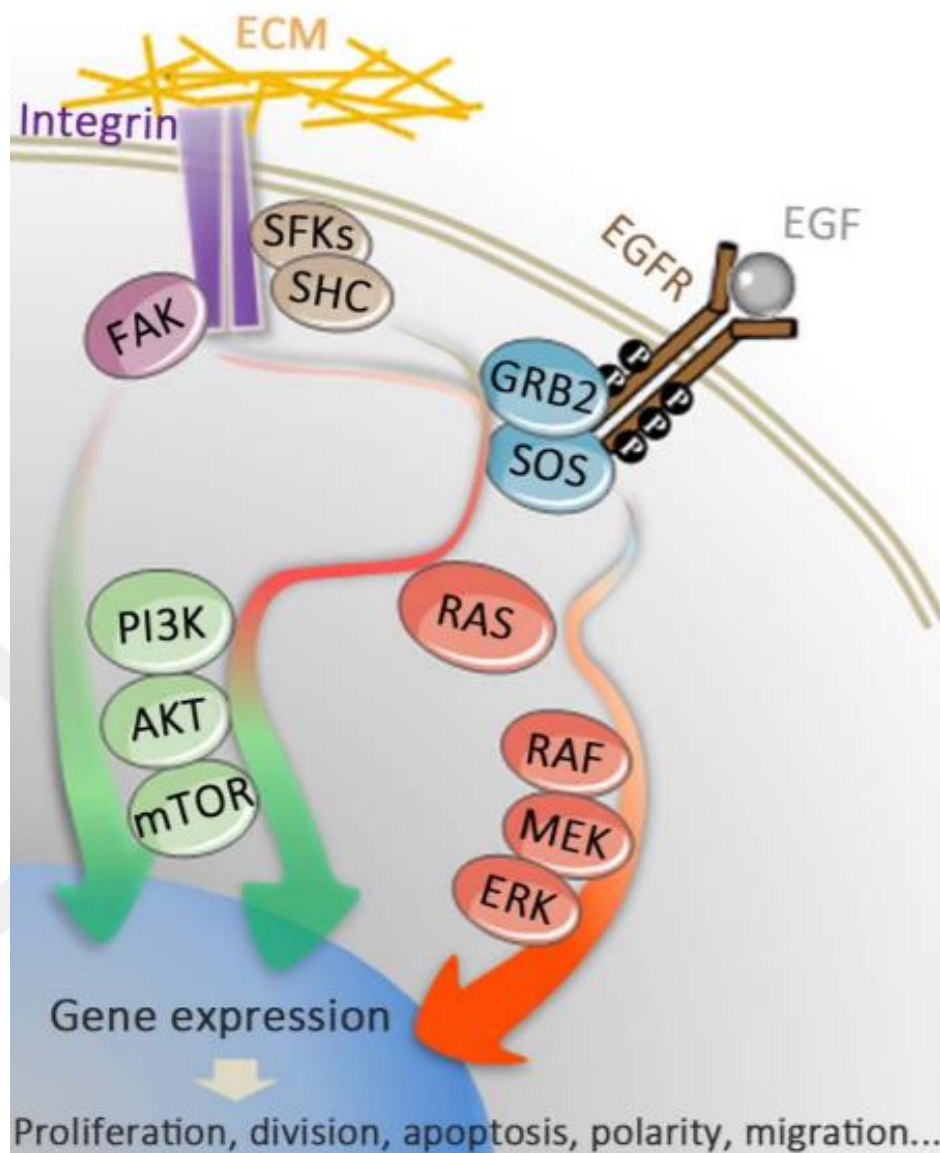


Figure 2.5: Overview of integrated relation of integrin, receptor tyrosine kinase epidermal growth factor (EGFR), RAS, MAPK and PI₃K-Akt signaling pathways. Activation of EGFR upon its ligand binding activates growth factor receptor-bound protein 2 (GRB2) and son of sevenless (SOS) interaction. The formation of the GRB2-SOS complex further activates RAS, downstream effector of EGFR signaling. RAS activation triggers signaling cascade involving MAPK (RAF-MEK-ERK) and PI₃K-AKT pathways. In addition to EGFR activation, integrin-ECM interaction could recruit these signaling cascades through the activation of FAK and SFKs (36).

2.8 Cell Immortalization

Primary cells are not capable to divide indefinitely. The nature of normal cells either in humans or mice are started to die after certain point due to intrinsic anti-tumorigenic mechanism. The mechanism behind this is replicative senescence (37, 38). During cellular division, each division ends up with telomeres shortening and after a certain point; telomeres become too short so; they can no longer able to shorten. During this stage, cells undergo senescence. Although, mouse cells have longer telomeres compare to human cells, they still can undergo stress-induced senescence. It is not impossible overcome stress factor with perfect growing conditions however; providing perfect conditions for every time is challenging thus, genetic modifications are necessary (37).

To eliminate further division, gatekeeper proteins p53 and pRB are responsible to detect these cells to induce their growth arrest. Certain stimulus can activate p53 and pRB pathways to drag cells to cell cycle arrest. To become mortal, cells need to escape from senescence. To achieve this, certain conditional immortalization techniques are valid and one is through the incorporation of simian virus 40 (SV40) large T viral antigen (37).

The responsiveness of SV40 mediated immortalization in rodent cells is around 100% compare to human cells (37). That is why we decided to use SV40 in our project. Simian virus 40 (SV40) large T expression in cells triggers the DNA synthesis both in actively dividing cells and in senescent cells. Large T capable to bind both pRB and p53, upon its binding it inactivates these proteins to overcome senescence activity (38).

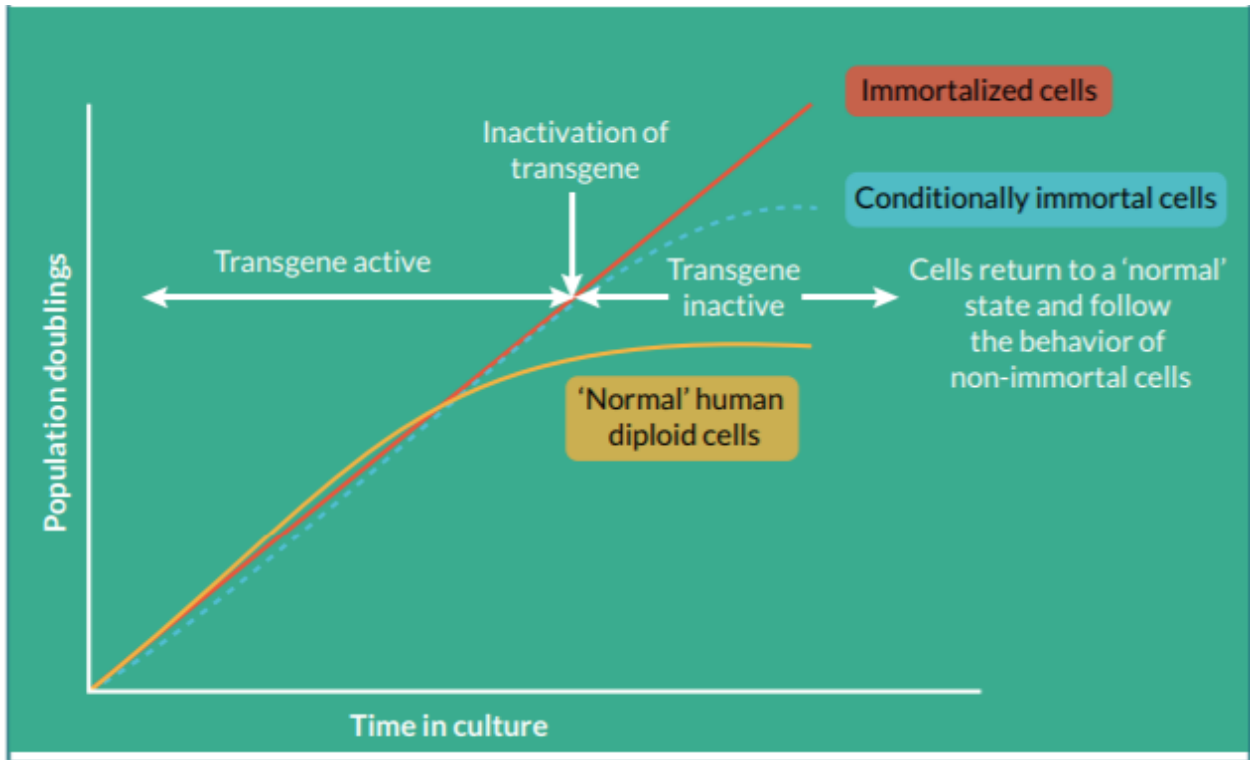


Figure 2.6: Schematic illustration of extended cellular lifespan via conditional immortalization technique.

3. MATERIAL AND METHODS

3.1 Type of Research

This study is an in vivo and in vitro experimental study.

3.2 Time and Place of Research

All experiments were conducted in between December 2016 - June 2019 in Izmir International Biomedicine and Genome Institute (IBG-Izmir).

3.3 Universe and Sample of Research

In this thesis project, human samples were not used.

3.4 Materials of Research

In this study, primary adult mouse lung cells were used and these cells were obtained from C57B/6 mice (IBG-Izmir animal facility) by us on various times. Table 3.1 provides detailed information about mice numbers and their usage dates. The isolation method is described in Data Collection Methods part.

Table 3.1: Mice types and numbers that were used in experiments are given with their dates.

Date	Mice Number	
12.12.2018	4	C57B/6
26.12.2018	5	C57B/6
07.01.2019	8	C57B/6
29.01.2019	6	C57B/6
18.03.2019	4	C57B/6
16.04.2019	4	C57B/6
18.04.2019	2	C57B/6
07.05.2019	6	C57B/6

3.5 Variables of Research

HITES medium, complete DMEM medium, Fetal Bovine Serum (FBS) and Penicillin-Streptomycin (Pen-Strep) ratio, plasmid are independent variables.

Mice species, cell-seeding density, antibody amounts and concentrations, amount of plasmid DNA are dependent variables.

3.6 Data Collection Methods

Table 3.2: HITES medium content

	Final concentration in 500 ml medium
FBS	10%
Human Epidermal Growth Factor (Human EGF)	0,000001mg/ml
Hydrocortison	10nM
Insulin transferrin selenium (ITS)	1X
Pennicilin-Streptomycin	100U/ml
Plasmocin	0,00625 µg/ml
RPMI 1640	1X
Sodium Pyruvate	0,5mM
β-estradiol	10nM

Table 3.3: Antibody cocktail content

	Antibody	Concentration	Catolog number	Brand
Primary	APC anti-mouse CD11c Antibody	1:200	117310	BioLegend
Primary	PE anti-mouse/human CD11b Antibody	1:800	101207	BioLegend
Primary	APC anti-mouse F4/80 Antibody	1:200	123116	BioLegend
Primary	Purified anti-mouse CD45 Antibody	1:500	103101	BioLegend
Primary	Purified anti-mouse CD16/32 Antibody	1:500	101301	BioLegend
Primary	CD19 Monoclonal Antibody (eBio1D3 (1D3)), PE, eBioscience™	1:800	12-0193-82	Invitrogen
Secondary	Goat anti-Rat IgG (H+L) Cross-Adsorbed Secondary Antibody, PE	1:500	A10545	Invitrogen

3.6.1 Animal Experiments

Mouse lung cells were obtained from wild-type (WT) C75BL/6 mice. Mice were housed and maintained by IBG Vivarium core facility. Mice were housed at 22-23°C room temperature, 40-70% humidity, 10 hour day/14 hour night photoperiods and individually ventilated cage conditions. Nutritional conditions were ad libitum. Commercial pellet feeds were used all feeds and water were sterilized.

3.6.2 Lung Cell Isolation

The following protocol for Clara cell isolation is based on Wang, Keefe, Jensen-Taubman, Yang, Yan and Linnoila (39) article and for the isolation of Alveolar type II cells Gereke, Autengruber, Grobe, Jeron, Bruder and Stegemann-Koniszewski (40), Sinha and Lowell (41) are used as reference protocols.

3.6.2.1 Preparation of the Mouse Lung

The mouse was sacrificed by CO₂ asphyxiation. The mouse was pinned down onto dissection tray and the ventral surface was sprayed with 70% alcohol. Ventral fur was removed by making a long cut along the ventral midline of the body. A sequential cut opened the peritoneum. Upon removal of fur and skin, rib cage was dissected to expose the heart and lungs without touching blood vessels. Inferior vena cava (IVC) near kidneys was snipped to exsanguinate the mouse. 10 ml syringe was filled with phosphate buffered saline (PBS) and the needle was inserted into the right ventricle of the heart in the direction of the pulmonary artery. Lungs were perfused upon PBS instillation. The heart was removed at the end of perfusion. After that, point salivary glands and the tissue-covering trachea were dissected to expose trachea. Trachea should not be damaged. By making a small cut on the ventral surface of the trachea, a 20G catheter was inserted into the trachea.

3.6.2.2 Enzymatic Digestion of the Lung Tissue

One ml syringe was filled with 1 ml collagenase/dispase and instilled into the lung through the catheter slowly until the lung lobes were fully expanded. Then syringe was exchanged with another syringe containing 0.5ml liquefied 1% low melting agarose (42°C) and instilled into the lung. The syringe was left in place and lungs were covered with ice to allow the agarose to solidify. Lungs were displaced and washed with PBS to eliminate remaining blood. If lungs are kept for a while, displaced lungs should be put in a falcon tube containing RPMI.

For Clara cells

After collecting the desired amount of lung, lungs were placed in 100µm cell strainer which in turn placed in glass petri. Lungs were minced with scissors into small pieces (1mm³) and 2 ml collagenase/dispase solution in PBS (per lung) was added onto the lungs. Lungs were incubated on a shaker for an hour at 37°C and 90 rpm.

For Alveolar type II cells

Collected lungs were transferred into 50 ml falcon tube containing 2ml collagenase/dispase solution in PBS (per lung). Allowed them to incubate for 45 minutes at room temperature and 150 rpm on a rocker.

3.6.2.3 Preparation of the Lung Cell Suspension

For Clara cells

After incubation, strainer was put on a 50 ml falcon tube and lungs were smashed by using the blunt end of the injector pressure pump to release cells. The remaining solution in the glass petri was collected and added into the same falcon. The suspension was filtered through 70 μ m and 40 μ m strainers sequentially. During this stage, strainers should be rinsed with two ml PBS with 3% FBS solution. After filtering, the cell suspension was centrifuged at 1400 rpm for 10 minutes. The supernatant was discarded and the pellet was resuspended in 2 ml Ammonium-Chloride-Potassium (ACK) lysis buffer for three to four minutes. Lysis was terminated by addition of 10 ml complete DMEM (DMEM with 10% FBS, 1% Pen-strep, 10mM HEPES). The cell suspension was centrifuged at 1400 rpm for 10 minutes and again the supernatant was discarded. The cell pellet was resuspended in 10 ml complete DMEM and the cell suspension was put in 10 mm petri dish and placed into an incubator at 37°C for 18 hours.

For Alveolar type II cells

After incubation lungs were transferred into a 10cm petri dish containing 7ml complete DMEM and 100 μ l DNase (1mg/ml). Intact lung tissue was pulled apart gently with fine forceps and allowed another 10 minutes for more cell release on a rocker. After incubation, a 100 μ m strainer was put onto 50 ml falcon tube then lungs and the cell suspension was put into the strainer. Lungs were smashed by using the blunt end of the injector pressure pump to release cells. The suspension was filtered through

70µm and 40µm strainers sequentially. During this stage, strainers should be rinsed with two ml complete DMEM. After filtering, the cell suspension was centrifuged at 300 g for 10 minutes at 4°C. The supernatant was discarded. and the pellet was resuspended in 2 ml ACK lysis buffer for three to four minutes. Lysis was terminated by addition of 10 ml complete DMEM. The cell suspension was centrifuged at 300 g for 10 minutes at 4°C.

3.6.2.4 Antibody Staining for Flow Cytometric Cell-Sorting

For Clara cells

After 18 hours incubation, recovered cells were trypsinized with Trypsin-EDTA solution and then, counted with hemacytometer. According to the number of the counted cells, the cell pellet was dissolved in PBS with 3% FBS and then distributed as 200 µl per well into V-bottomed 96 well plate. For Clara cells, rabbit anti-Clara Cell Secretory Protein Antibody (cat no 07-623, Millipore) was applied at 1:100 concentration and antibody-applied cells were incubated for an hour at dark on ice. During antibody staining control cells were remained in 200 µl PBS with 3%FBS. After incubation, cells were rinsed in PBS with 3% FBS and centrifuged for five minutes at 800g. The supernatant was discarded and the pellet was resuspended in 200µl PBS with 3% FBS. Secondary antibody staining was done with Alexa Fluor® 647-conjugated AffiniPure Donkey Anti-Rabbit IgG (H+L) (cat no 711-605-152, Jackson ImmunoResearch Laboratories) at 1:500 concentration. Primary antibody applied cells were stained with secondary antibody and incubated for an hour at dark on ice with controls. Incubated cells were rinsed in PBS with 3% FBS and centrifuged for five minutes at 800g. The supernatant was discarded and the pellet was resuspended in Fluorescence-activated cell sorting (FACS) buffer (1X PBS, 1mM EDTA, 25Mm HEPES, 1%FBS). Cells were stained with DAPI for five minutes (except unstained control). Then, cells were rinsed in FACS buffer and centrifuged for five minutes at 800g. After discarding supernatants, cell pellets were resuspended in FACS buffer and filtered

through 40µm filter cap FACS tubes. Cells were sorted with BD FACSAria™ III sorter in IBG flow cytometry core facility.

For Alveolar type II cells

The supernatant was discarded and the cell pellet was resuspended in 3ml antibody cocktail (Table 3.3) that prepared in 3ml complete DMEM. Cells were incubated in antibody cocktail solution on ice for 45-60 minutes. Control cells (unstained control and single-strained controls) should be separated before antibody staining and they should be treated in complete DMEM while sample cells are in antibody cocktail-DMEM solution. After incubation, the cell suspension was rinsed in 10ml complete DMEM and centrifuges for 10 minutes at 300g, 4°C. The supernatant was discarded and the pellet was resuspended in 3ml secondary antibody cocktail prepared in complete DMEM. Primary antibody applied cells were incubated on ice for 45-60 minutes at dark. Single-stained controls (except DAPI stained control) were prepared during secondary antibody application. Incubated cells were rinsed in 10ml complete DMEM and centrifuged for 10 minutes at 300g, 4°C. The supernatant was discarded and the pellet was resuspended in FACS buffer. Cells were stained with DAPI for five minutes (except unstained control). Then, cells were rinsed in FACS buffer and centrifuged for five minutes at 800g. After discarding supernatants, cell pellets were resuspended in FACS buffer and filtered through 40µm filter cap FACS tubes.

Cells (both Clara and AECII cells) were stained with DAPI for five minutes (except unstained control). Then, cells were rinsed in FACS buffer and centrifuged for five minutes at 800g. After discarding supernatants, cell pellets were resuspended in FACS buffer and filtered through 40µm filter cap FACS tubes.

3.6.3 Intracellular Staining For Flow Cytometry Analysis

Cells were plated out with StemPro™ Accutase™ Cell Dissociation Reagent (Cat No: A1110501, Thermo). Cells were counted with hemacytometer and distributed into V-bottomed 96 well plate and rinsed twice in PBS. The 96 well plate was centrifuged for 5 minutes at 400g and 4°C. Cells were stained with Zombie NIR (Cat No: 423105, BioLegend), (only Zombie single stained control and the sample) at 1:2000 concentration in PBS for 10 minutes. After 10 minutes, cells were rinsed twice in PBS. After centrifugation, cells were treated with CytoFix/CytoPerm buffer (Cat No: 554722, BD, 150µl/well) for 10 minutes at dark. At the end of the buffer treatment cells were rinsed twice in BD Perm/Wash (Cat No: 554723, BD). Then the well plate was centrifuged for 5 minutes at 400g and 4°C. The supernatant was discarded and the sample was treated with the appropriate primary antibody (anti-proSP-C at 1:200 and anti-CCSP at 1:100) diluted in Perm/Wash for overnight at 4°C. During this stage control cells were kept in PBS with 3% FBS. After overnight incubation in primary antibody, cells were rinsed twice in Perm/Wash and then incubated with appropriate secondary antibody (Alexa Fluor® 647 at 1:500 concentration) diluted in Perm/Wash for 30 minutes at room temperature at dark. After incubation, cells were rinsed twice in Perm/Wash. Then cells were resuspended in FACS buffer and filtered through 40µm filter cap FACS tubes for data acquisition. Data acquisition was performed on BD LSR FORTRESSA cell analyzer in IBG flow cytometry core facility. Acquired data was analyzed on FlowJo software.

3.6.4 Immunofluorescence Experiment

Sterilized 12 mm glass coverslips were placed in 24-well culture plates. Lung cells were plated on coverslips as in 125×10^3 cells per well and incubated overnight. After incubation, the medium was removed and cells were rinsed gently for three times in ice-cold PBS. Cells were fixed within 500µl 4% formaldehyde in PBS solution and then left for 15 minutes incubation at room temperature. Subsequently, fixative was removed and cells were rinsed for three times in ice-cold PBS. Cells were kept within

0.1% Triton[®] X-100 Surfact-Amps[®] Detergent Solution (Prod #85112, Thermo Scientific) in PBS solution for 15 minutes at room temperature. Then cells were rinsed gently for three times in-ice cold PBS. To eliminate non-specific binding, 500 µl 2% BSA in 1X PBS solution was added onto cells and, cells were incubated at room temperature for an hour. After incubation, cells were rinsed three times in-ice cold PBS. In order to detect Clara cells, rabbit anti-Clara Cell Secretory Protein antibody was used at 1:100 in addition, for AECII detection, rabbit Anti-Prosurfactant Protein C (proSP-C) Antibody (cat no AB3786, Millipore) was used at 1:500. Anti-CCSP antibody and proSP-C was diluted in PBS and added onto cells. Cells were kept in the solution for an hour at room temperature in a humidified chamber. Alexa Fluor 647-conjugated antibody was used as secondary antibody at 1:500 concentration. Alexa Fluor[®] 647 antibody was diluted in 500 µl PBS and added onto cells. Cells were kept in the secondary antibody for an hour at room temperature in a humidity chamber at dark. Afterwards incubated cells were washed three times in ice-cold PBS at dark. 5 µl 1 µg/ml DAPI was added to stain nucleus and incubated for two minutes at dark. Cells were washed three times in ice-cold PBS at dark. Coverslips were displaced gently and placed onto microscope slides reversibly. Slides were examined under OLYMPUS IX71 Fluorescence Microscope that resides in IBG Core Facility. Randomly chosen fields under the microscope were visualized and their pictures were taken. Taken pictures were analyzed with ImageJ program.

3.6.5 Immortalization of cells

3.6.5.1 Plasmid Preparation and Transformation

100 µl aliquoted DH5α competent cells were thawed on ice. 1 µl pBABE SV40 puro plasmid (Figure 3.1) diluted in 9 µl distilled water (1:10) and mixed with 100 µl competent cell in 1.5 ml eppendorf. The mixture was incubated for 30-40 minutes on ice. The mixture was treated with heat in 42°C water for 90 seconds then, immediately put on ice for two minutes. The cell-plasmid suspension was added into 900 µl pre-warmed LB broth medium and incubated at 37°C at 225 rpm for an hour. 100 µl of the

suspension was plated onto LB Agar plates with antibiotics in a drop-wise manner. The remaining solution was centrifuged at 8000 rpm for five minutes. The supernatant was discarded and the pellet was resuspended in 100 µl LB broth medium. The suspension was plated onto LB Agar plates with antibiotics in a drop-wise manner. Plates were put into incubator reversibly after 15 minutes and left overnight incubation at 37°C. After colony formation, single colonies were selected and cultured into five ml ampicillin added LB broth medium for overnight at 37°C. Two ml of culture was inoculated in 200 ml ampicillin added LB broth for overnight at 37°C.

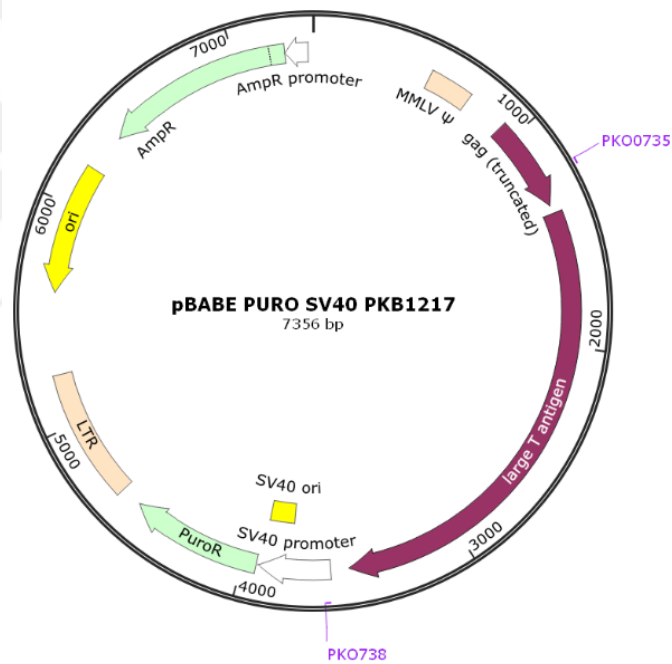


Figure 3.1: pBABE SV40 puro PKB1217 plasmid map which was taken from SnapGene Viewer.

3.6.5.2 Plasmid DNA Isolation (Maxi Prep)

QIAGEN® Plasmid Maxi Kit (25) (Cat no 12163) was used and its protocol was carried out with slight changes.

The concentration of DNA was measured with Nanodrop. Approximately 12,000 ng/μl DNA was obtained. Further, we diluted the DNA to 3000 ng/μl upon addition of 300 μl TE buffer.

3.6.5.3 Preparation of PLAT-E Cells

Plated Platinum-E (PLAT-E) cells were taken from Diril Lab in a T25 flask. These cells were further cultured by us. Culture media for PLAT-E cells including; high glucose DMEM (1X, cat no 41965-039 500 ml, Gibco), 10% FBS, 1μg/ml puromycin (10 mg/ml, cat no ant-pr-1, InvivoGen), 10μg/ml blasticidin and 1% Penicillin-streptomycin (Pen-Strep, cat no 15140-122 100 ml, Gibco).

3.6.5.4 Transfection

XTremeGENE 9 DNA Transfection Reagent (REF 06365787001, Roche) was diluted with OPTI-MEM (1X, Reduced Serum Medium, REF 31985-062, Gibco) medium to a concentration of 3 μl reagent /100 μl (3:1). 1μg pBABE SV40 puro DNA was added into OPTI-MEM:XTremeGENE Reagent mixture, and incubated for 15 minutes at room temperature. After incubation, 500 μl of DNA mixture was added to PLAT-E cells in a dropwise manner. Then, petri was gently shaken and left for incubation at 37°C. After 48 hours, medium-containing viruses were collected and filtered through 0.22 mm strainer. 1ml aliquots were made and stored at -20°C.

3.6.5.5 Viral Transduction

Isolated lung cells were plated with HITES medium (Table 3.2) into 25T flasks. After 24 hours (when cells reach to 60% confluency), 400 μ l virus supernatant was mixed with 1600 μ l 8 μ g/ml polybrene containing growth medium and added onto cells gently.

3.6.5.6 Puromycin Selection

3 mg/ml puromycin was used for selection from 10mg/ml puromycin stocks. The old medium was replaced with fresh medium every three days. Then, cells were trypsinized and plated into a T25 flask.

3.7 Research Plan

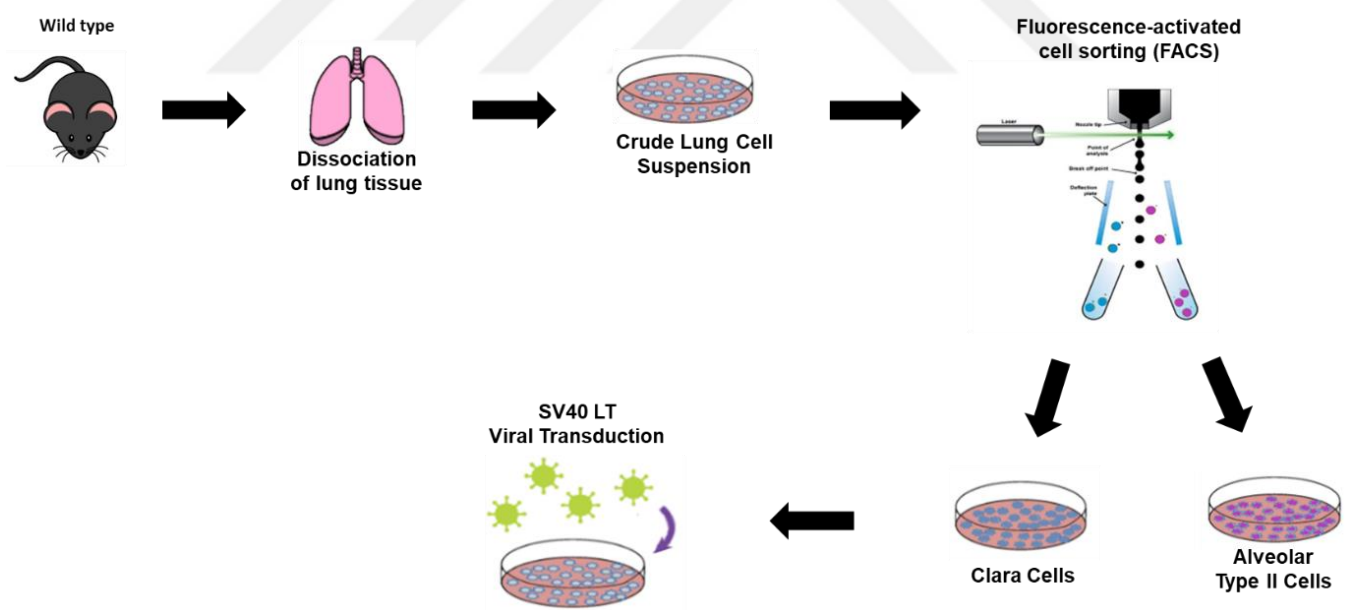


Figure 3.2: Illustration of initial experimental procedure.

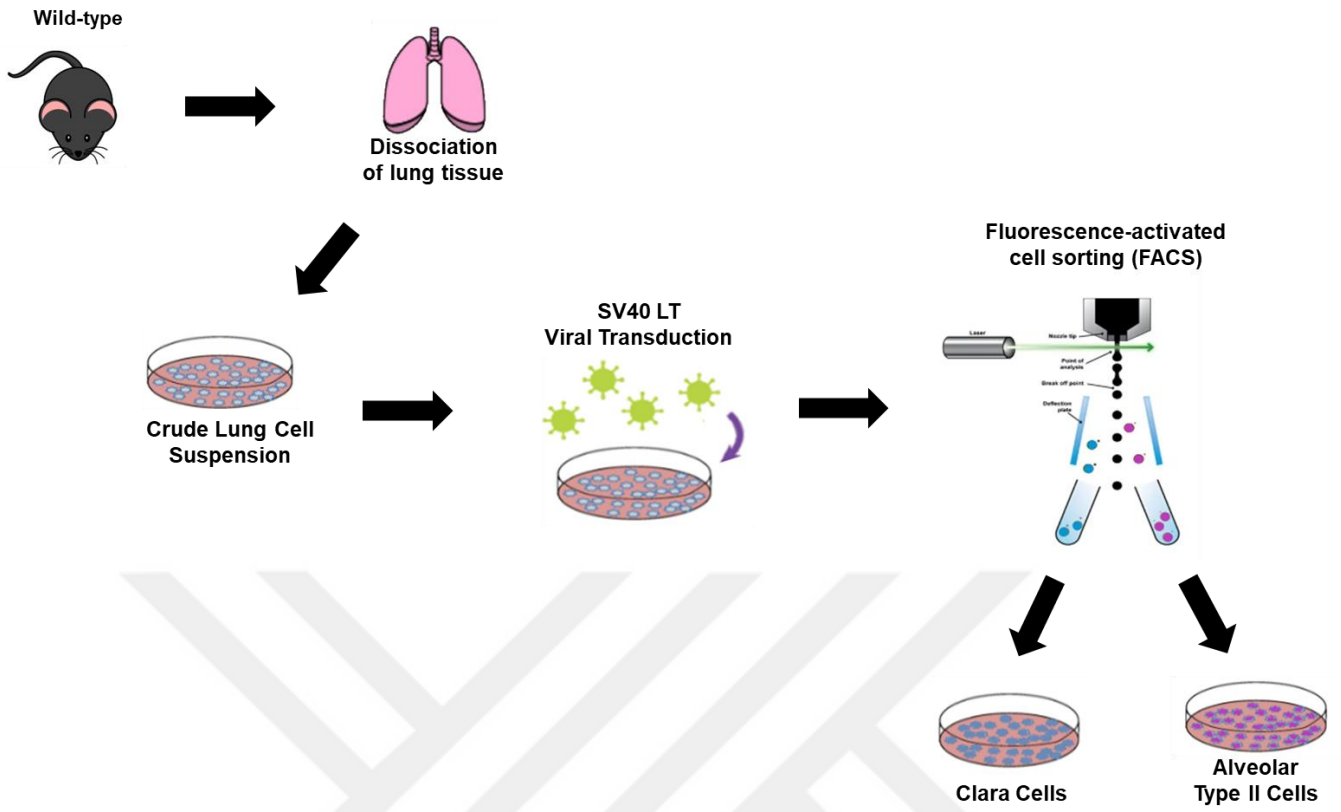


Figure 3.3: Illustration of second experimental procedure.

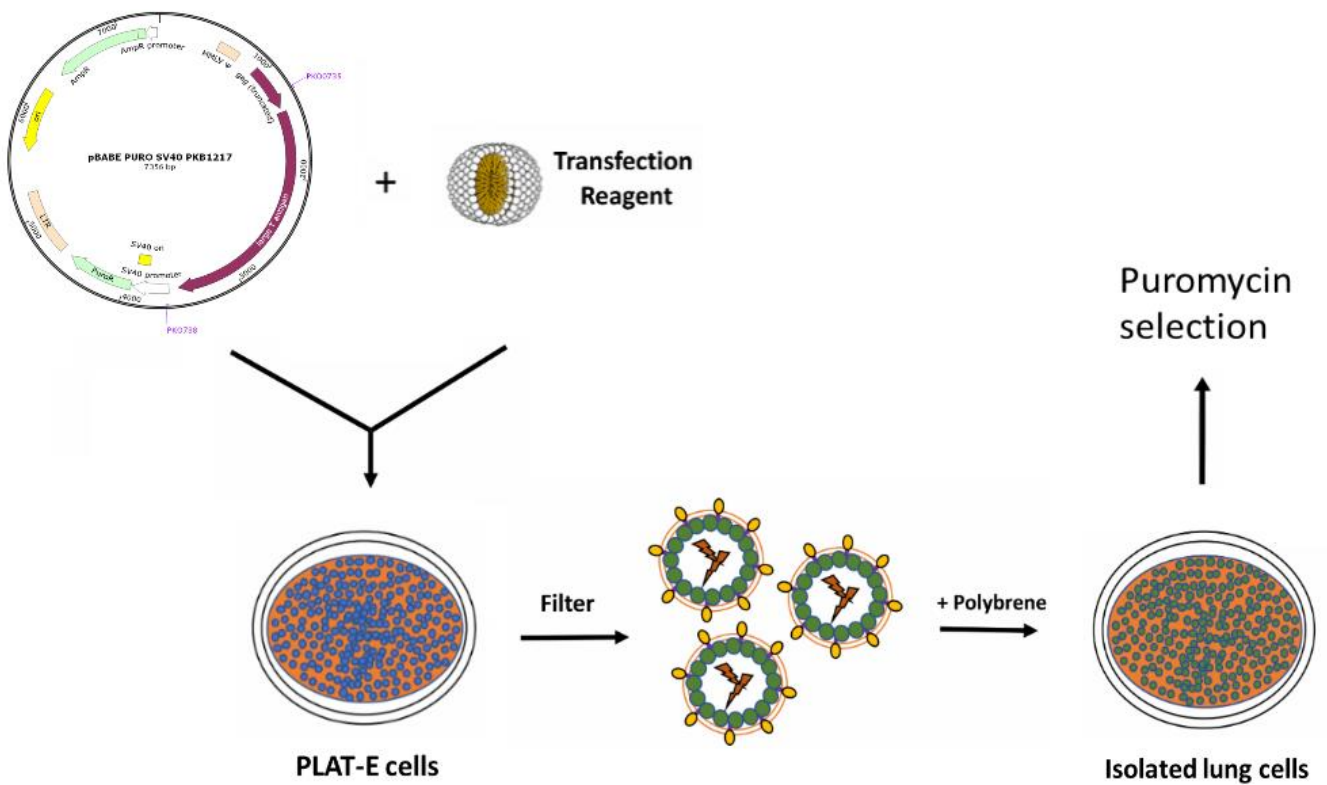



Figure 3.4: Schematic view of immortalization procedure.

Our work plan illustration was given in Figure 3.2. In Figure 3.3, the revised version of our work plan was given. In Figure 3.4, experimental design of immortalization was given.

3.8 Limitations of Research

If we fail to obtain primary Clara cells and alveolar type II cells, mouse embryonal fibroblast (MEF) cells will be used. In case of having problems during fluorescence-activated cell sorting, cells will be immortalized first and then they will be sorted.

3.9 Ethical Committee Approval

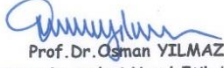
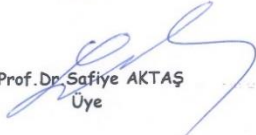

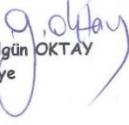

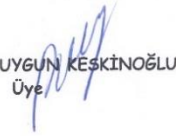


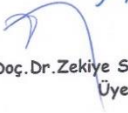
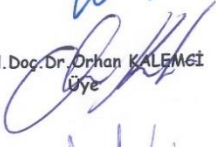
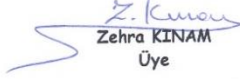
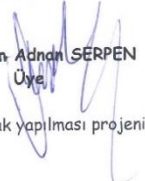
**DOKUZ EYLÜL ÜNİVERSİTESİ HAYVAN DENEYLERİ YEREL ETİK KURULU**

35340, İnciraltı, İzmir-232 4122234

Gündem No/ Toplantı No/Yılı : 04/04/2016
Toplantı Tarihi : 23 Şubat 2016

Sayın, Yard.Doç.Dr.Ralph Meuwissen
İzmir Biyotıp ve Genom Merkezi Kanser Biyolojisi Bölümü

07/2016 Protokol No'lu; yürütücüsü olduğunuz "Akciğer Kanseri Başlangıcı ve İlerlemesini Kontrol Eden Hippo Yolağının $\beta 1$ İntegrine Bağlı Regülasyonunun Fonksiyonel Analizi" isimli; Prof.Dr.Ensari GÜNELİ ve İzgi UÇER'in araştırmacı olduğu, 50 adet fare kullanılacak olan projenin uygulanmasında etik açıdan sakınca olmadığına oy birliği ile karar verilmiştir.
Bilgilerinizi ve gereğini rica ederiz.

 Prof. Dr. Osman YILMAZ Hayvan Deneyleri Yerel Etik Kurulu Başkanı	Prof. Dr. Ali Necati GÖKMEN Başkan Vekili
 Prof. Dr. Safiye AKTAŞ Üye	 Prof. Dr. Hüsnü Alper BAĞRIYANIK Üye
 Prof. Dr. Gülgün OKTAY Üye	Prof. Dr. Hatice Nur OLGUN Üye (Topl. katılmadı)
Prof. Dr. Mehmet Ensari GÜNELİ Üye(Araştırmacı)	Prof. Dr. Günay KIRKIM Üye(Topl. Katılmadı)
 Doç. Dr. Meral KARAMAN Üye	 Doç. Dr. Pembe UYGUN KEŞKİNOĞLU Üye
 Doç. Dr. Türkan ERTAY Üye	 Doç. Dr. Nermin Nüket GÖCMEN MAS Üye
 Doç. Dr. Zekiye Sultan ALTUN Üye	 Yard. Doç. Dr. Orhan KALEMÇİ Üye
 Zehra KINAM Üye	 Vet. Hekim Adnan SERPEN Üye

NOT: Projede yapılan düzeltmelerin metin içinde bold karakter kullanılarak yapılması projenin incelenmesi açısından sağlıklı olacaktır.

4. RESULTS

We purified Clara and Alveolar type II cells from total lung epithelial cell mixtures by flow cytometry-based cell sorting techniques. Each cell types require its own procedure for obtaining a high yield. In order to isolate Clara cells, crude lung cell suspension should be left for recovery for 18 hours and then cells should be prepared for sorting experiment. CCSP is a well-known Clara cell marker and we used an anti-CCSP polyclonal Ab for Clara cell purification. In order to be capable of working with mutant mice, first we need to optimize the whole isolation process since we do not have too many mutant mice and any mistake may end up with undesirable results. Since AECII isolation protocol is a negative selection which necessities more than two antibodies utilization and in order not to waste antibody we started with Clara cells. More importantly, isolation of two distinct cell types signifies a need for extra mice and to reduce the number of mouse consumption, we decided to initially optimize Clara cell isolation.

4.1 Clara cell isolation and immunofluorescence experiment

Wang et al. were able to isolate Clara cells by using flow cytometry and our protocol for Clara cells is based on their paper. The schematic overview is presented in Figure 4.1 (39).

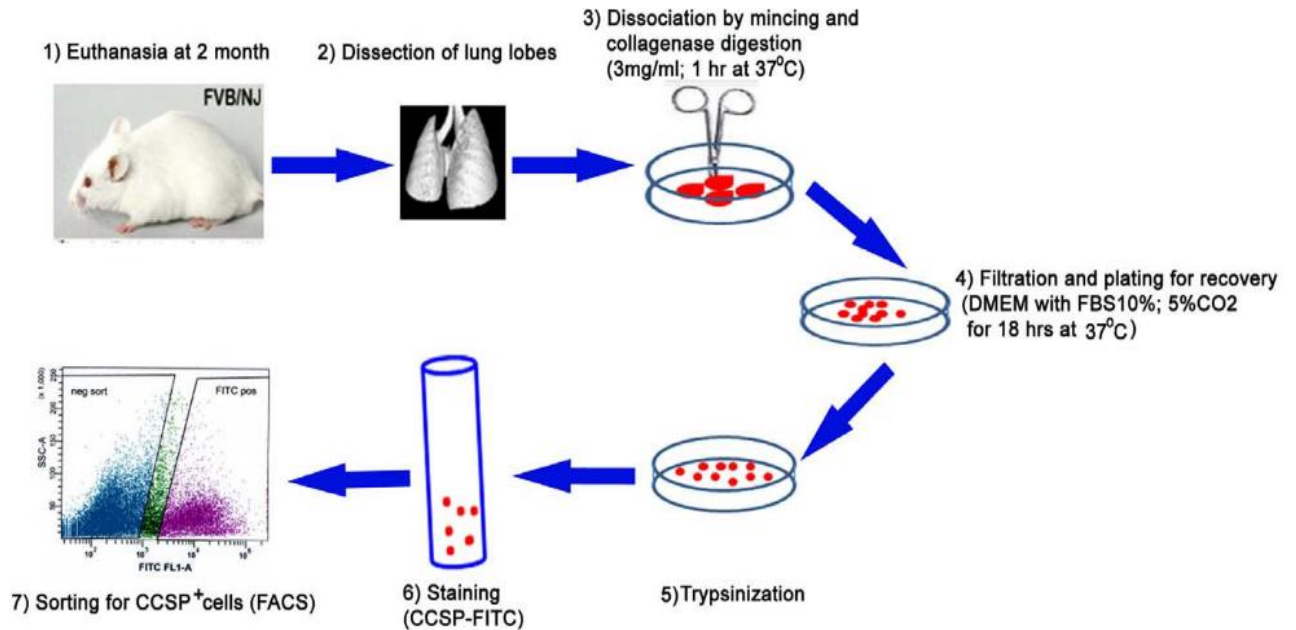


Figure 4.1 Schematic overview of isolation protocol for CCSP positive cells from mouse lung (39).

Consistent with our reference paper we performed isolation method at different time points. However, during the experiment, we confronted different problems.

Initially, the purity of CCSP⁺ cell population was good (Figure 4.2) however, the number of cells was not enough to proceed with further experiments.

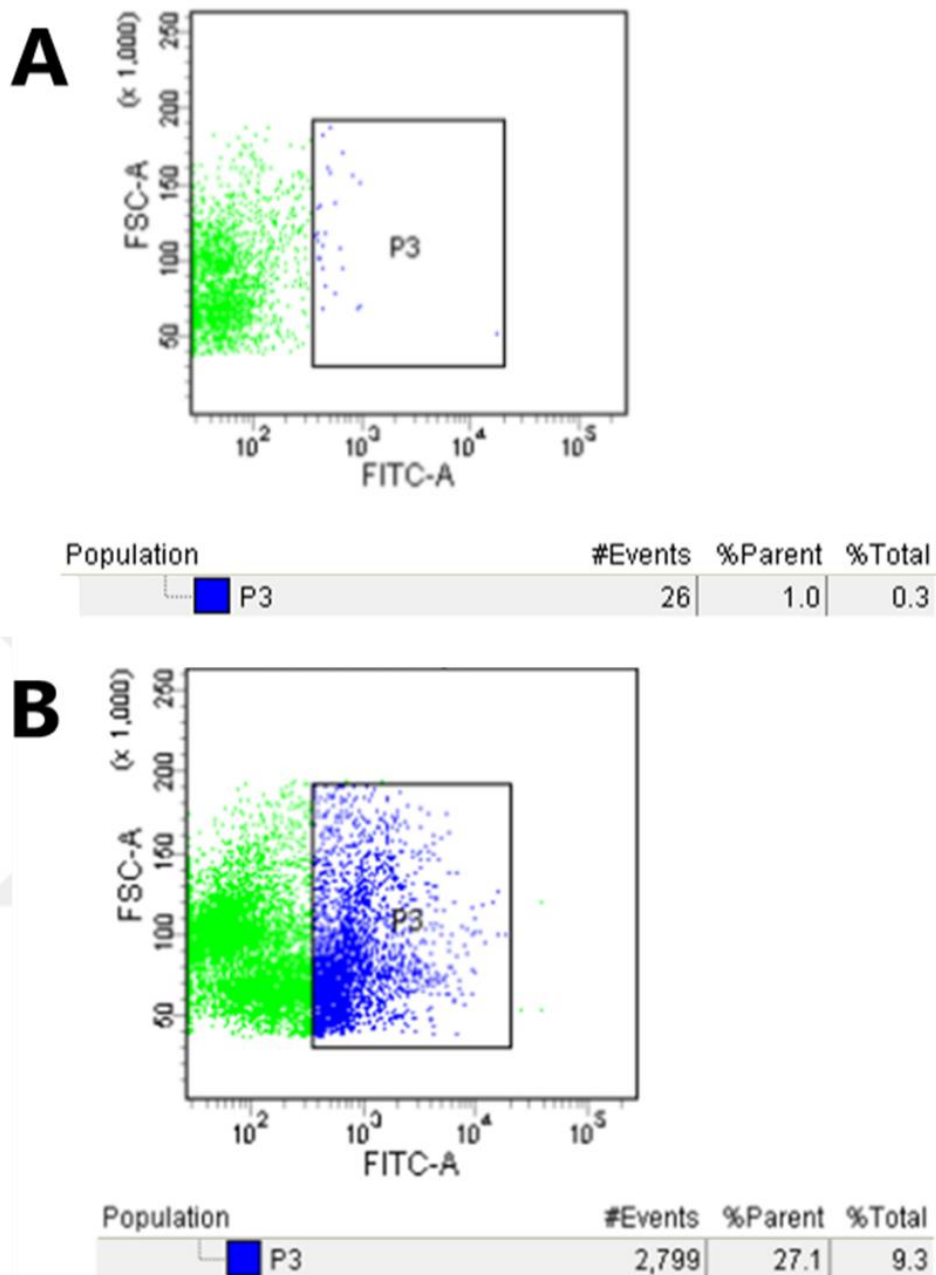


Figure 4.2 Sorting data of total lung cells. **A.** Crude lung cells were only incubated with secondary antibody goat anti-rabbit FITC. To discriminate dead/alive cells, cells were stained with DAPI. **B.** The whole lung cell suspension was incubated with CCSP primary antibody during an one-hour incubation; secondary antibody goat anti-rabbit FITC incubation was performed. Again to discriminate dead/alive cells, cells were treated with DAPI. After several gating processes, P3 was chosen as FITC positive population that represents CCSP⁺ cells.

Afterward, we decided to increase the number of mice to attain sufficient cells after sorting.

However, even though we had a great number of cells before sorting (Figure 4.3), we were confronted with a shifting problem during sorting (Figure 4.4).

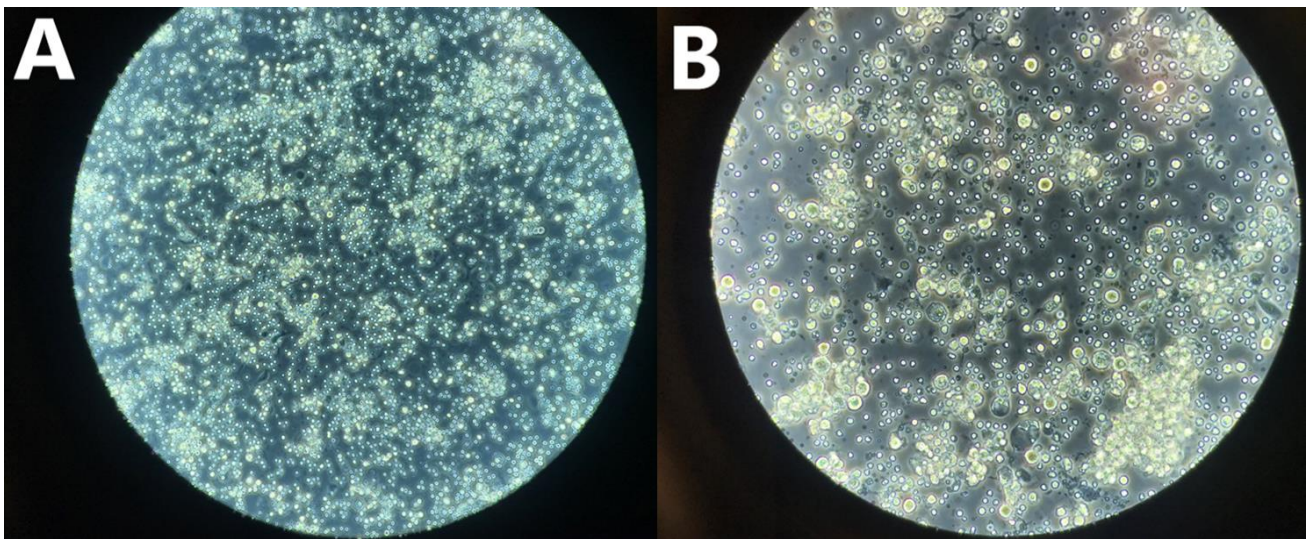


Figure 4.3 Microscope images of cells after ACK lysis buffer treatment and before sorting **A.** 10x magnification of lung cells. **B.** 20x magnification of lung cells.

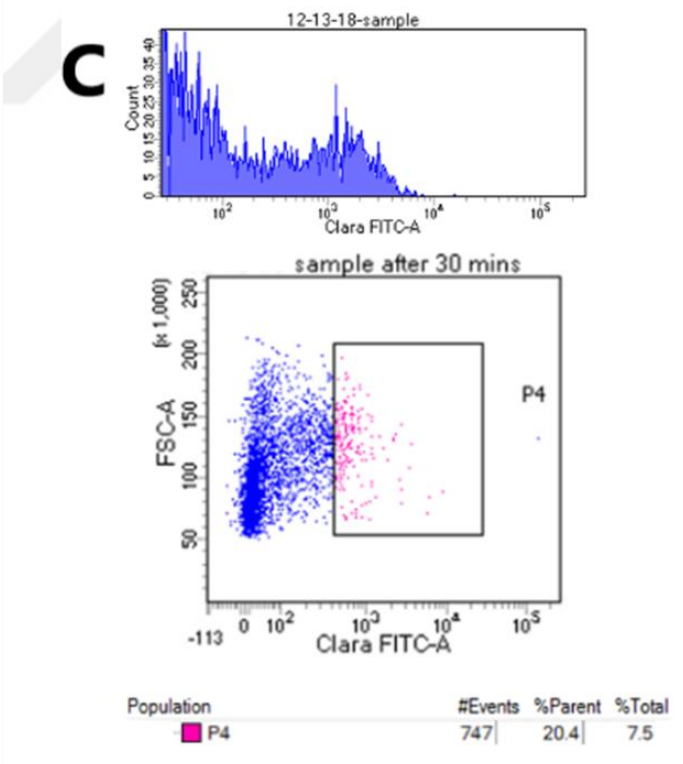
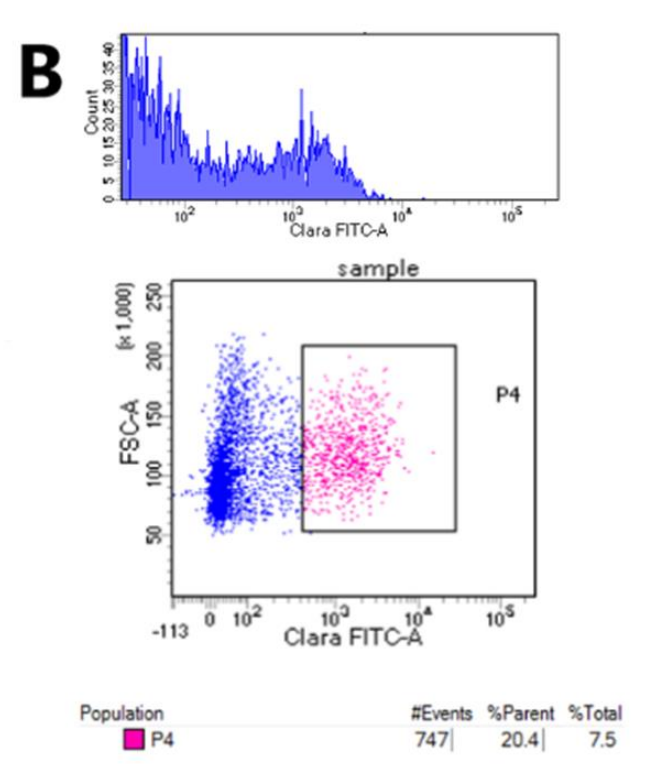
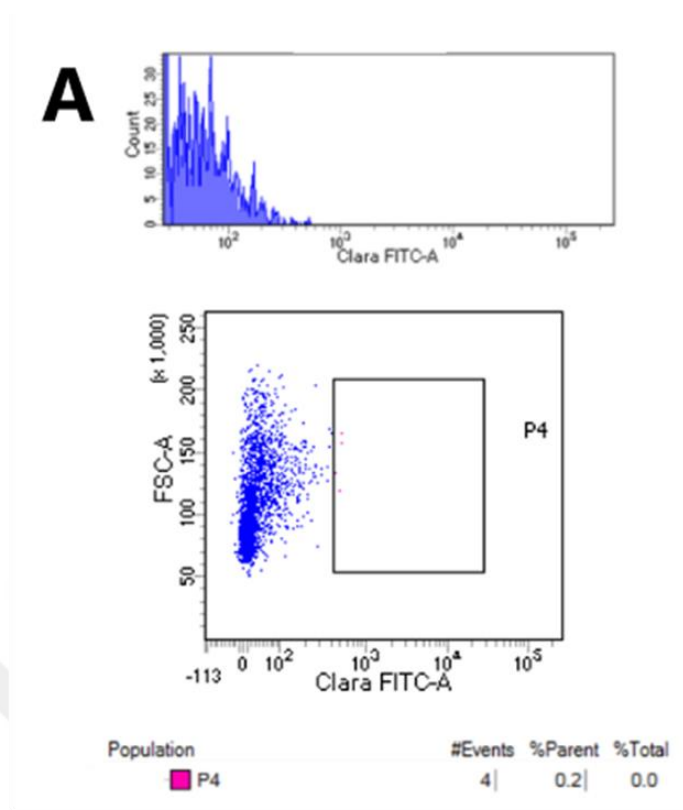


Figure 4.4 FACS ARIA III sorting result. **A.** Control cells were stained only with secondary antibody and DAPI. **B.** FITC histogram graph and FITC⁺ cell populations with percentage were given. **C.** Sample in A after 30 minutes. In histogram figure, a shift was observed in x-axis that results in a decrease of FITC⁺ population.

At the end of sorting, cell yield was too low to perform further experiments and when we tried to grow sorted cells, we saw that our primary cells rapidly died. Directly after sorting we supplemented cells with growth medium and put sorted cells into T25 flask to allow cell growth. However, three days later we observed that cells were not healthy as on the first day and they started to die (Figure 4.5).

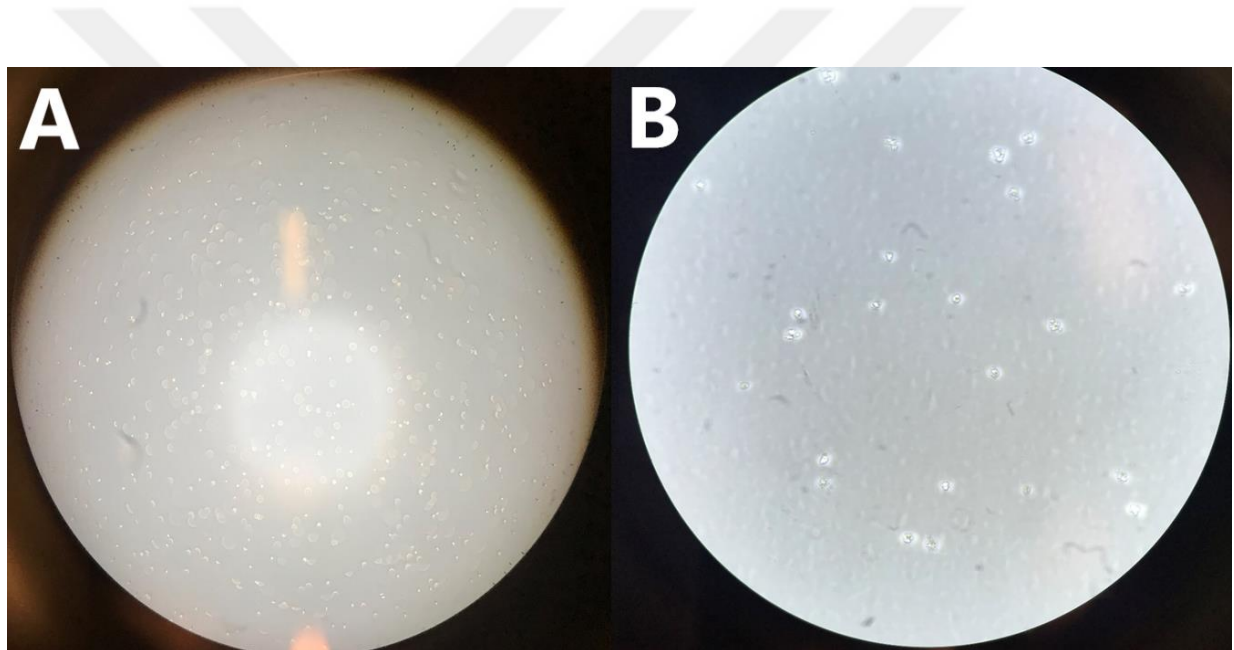


Figure 4.5 A. Sorted cells were put into a flask and supplied with HITES medium immediately after sorting. **B.** Cells three days after sorting.

To understand whether this shifting problem was a one-time problem originating from the device or was due to the loss of secondary antibody efficiency, we decided to use another secondary antibody Alexa Fluor[®] 647-conjugated AffiniPure Donkey Anti-Rabbit IgG (H+L) apart from Goat Anti-Rabbit IgG (H+L) Secondary Antibody FITC conjugated. During this experiment, we sacrificed eight mice to increase the yield. After ACK lysis buffer treatment, we counted cells and obtained

approximately 13 million cells. Since, after sorting, cells were no longer able to grow, we were doubtful about sorting machine damages our cells. Therefore, we used counted cells for both sorting and immunofluorescence experiments to verify the reliability of our results with different experiments.

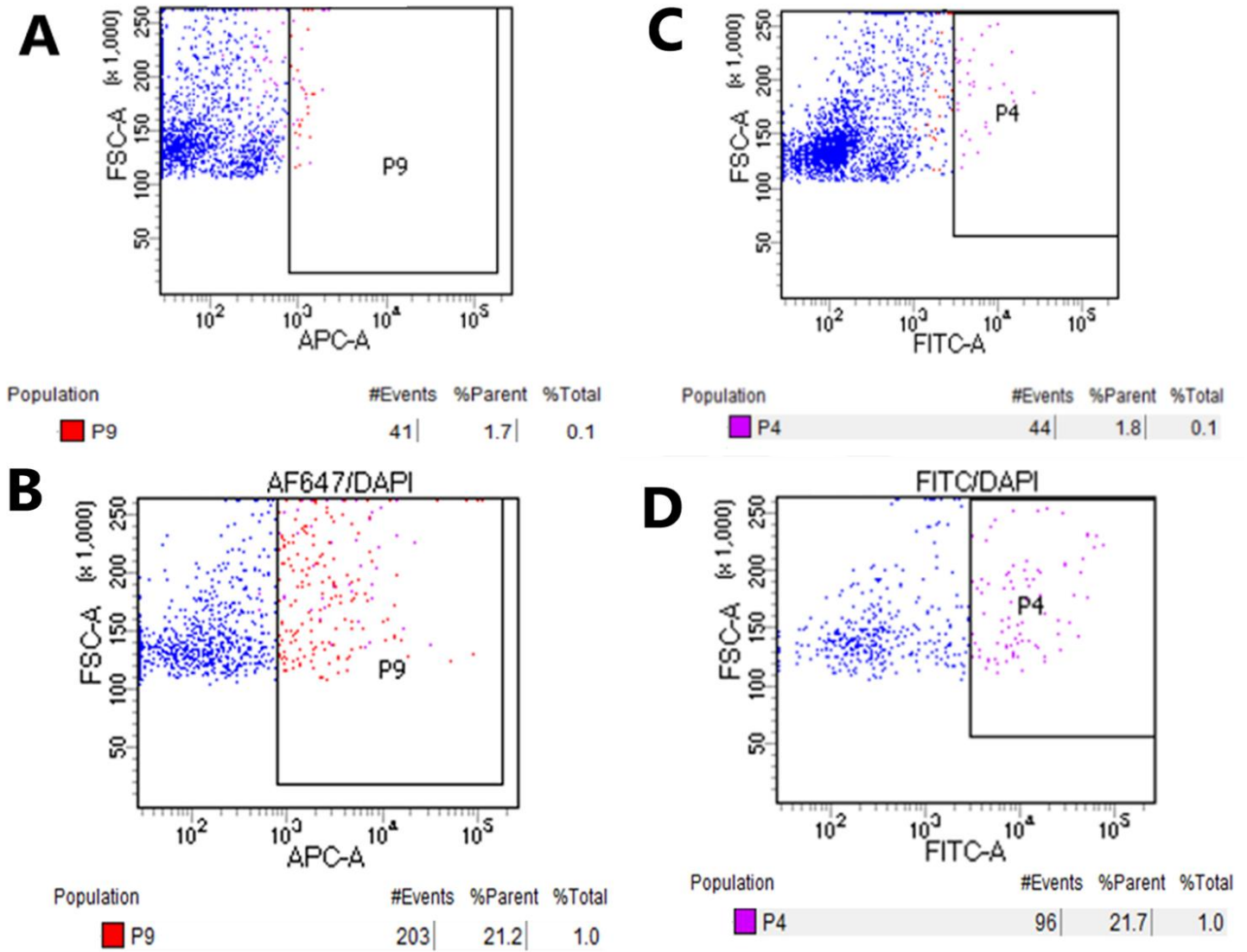


Figure 4.6 FACS ARIA III sorting result. **A.** Control cells were stained with Alexa 647 **B.** Anti-CCSP labeled Alexa 647⁺ cell population with percentage was given. **C.** Control cells were stained with FITC **D.** Anti-CCSP labeled FITC⁺ cell population with percentage was given.

Again after sorting, we had fewer cells than we expected however, we used all sorted cells for immunofluorescence experiment in order to compare Immunofluorescence (IF) data before and after sorting. In accordance with sorting results, we did not observe a significant difference between Alexa Fluor 647 and FITC also, we did not encounter with the shifting problem (Figure 4.6) and thus, maybe shifting problem was due to a machine-related problem. Nevertheless, we decided to use Alexa Fluor 647 as a secondary antibody.

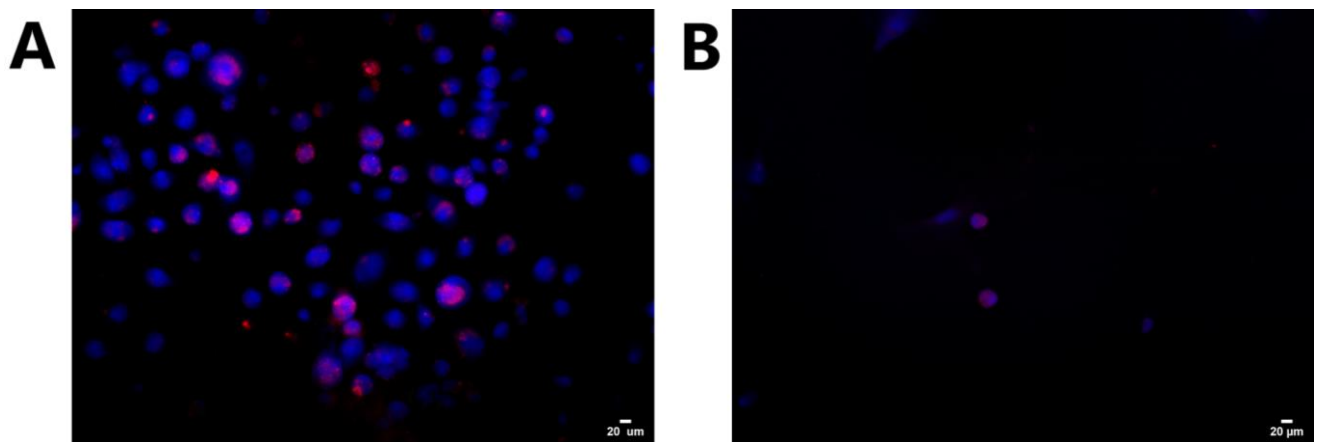


Figure 4.7 Immunofluorescence experiment images of labeled CCSP cells. **A.** Alexa Fluor 647 staining of CCSP labeled cells. After counting, unsorted cells were separated and plated onto coverslips for IF experiment. Images were taken two days after isolation in 40X magnification. **B.** Alexa Fluor 647 staining of sorted CCSP⁺ cells. CCSP⁺ cells were seeded onto coverslips for IF staining. Images were taken one day after sorting in 40X magnification.

According to IF images in Figure 4.7 we obtained, as expected, CCSP⁺ cells. However, we had a far higher number of CCSP⁺ cells in the unsorted total cell mixture. This meant that we were losing a significant amount of primary Clara cells during sorting with the FACS Aria III.

In accordance with our work plan in Figure 3.2, we were planning to isolate desired cells from our mutant mice and then, after culturing cells for a while, we would immortalize these cells. However, we could not achieve to isolate enough cells and

even we achieved this, cells did not survive long enough to immortalize them. So; we could not proceed with the follow-up experiments. For this reason, we decided to change our work plan into Figure 3.3, and to perform sorting experiment after primary cell immortalization.

4.2 Crude Lung Cell Immortalization

In order to immortalize cells, we took pBABE SV40 puro plasmid from Diril Lab and prepared according to 3.4.1 Plasmid Preparation and Transformation part. Then, we isolated plasmid DNA and transfected into PLAT-E cells, which were also taken from Diril Lab, by using XtremeGENE Reagent. Two days after transfection, we collected viruses. Collected viruses were transduced into crude lung cells. We obtained lung cells according to 3.6.2 Lung Cell Isolation method without performing antibody staining. Three days later, we applied puromycin to our transduced cells in order to select puromycin resistant cells. We started with 250ng/ml and 500ng/ml puromycin application (Figure 3.4).

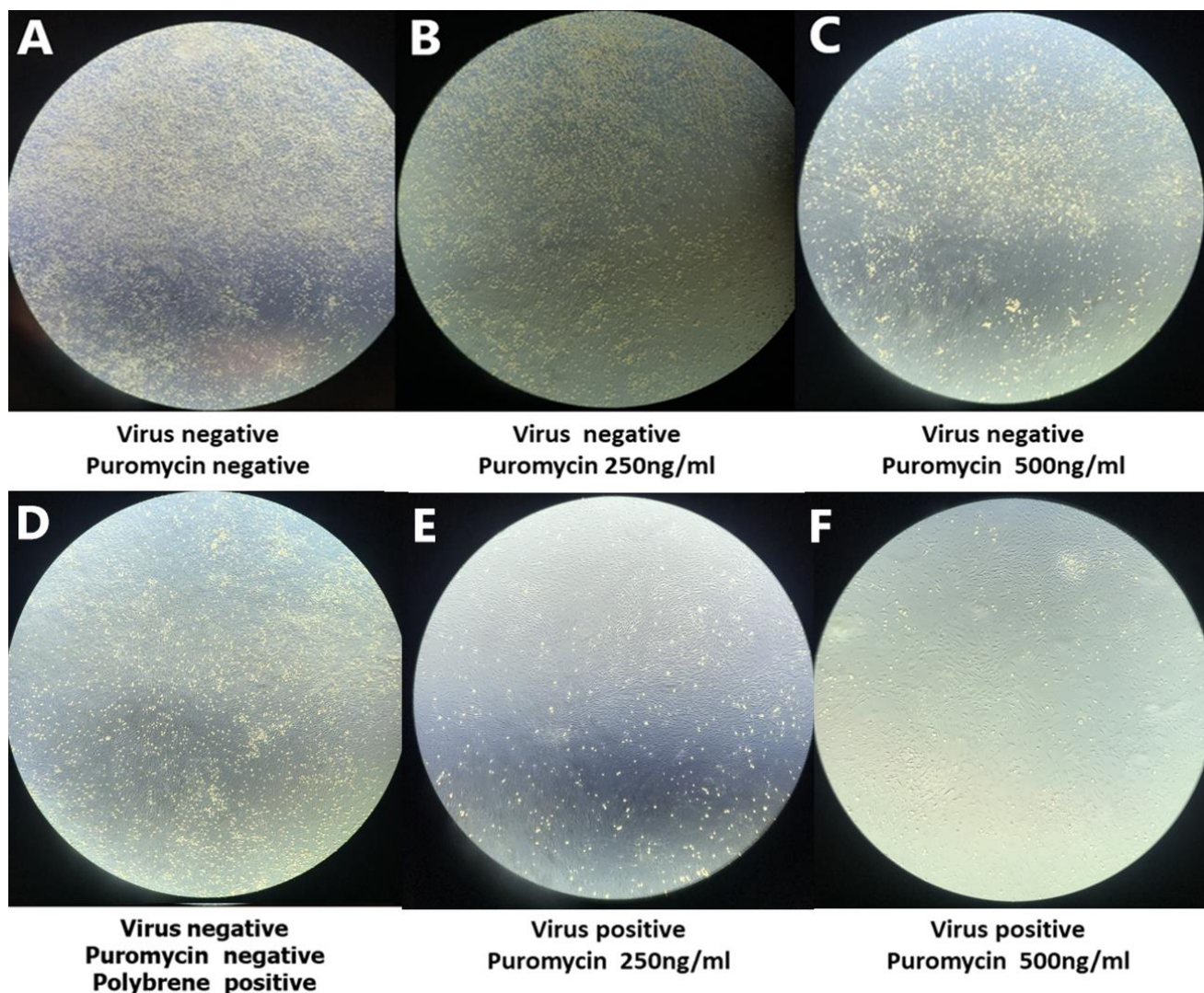


Figure 4.8: Determination of puromycin concentration for selection and control groups. Images were taken under 10x magnification. **A.** Control lung cells without viral transduction and without puromycin application. **B.** Untransduced lung cells with 250ng/ml puromycin application. **C.** Untransduced lung cells with 500ng/ml puromycin application. **D.** Polybrene control in untransduced and non-puromycin applied cells. **E.** Transduced lung cells with 250ng/ml puromycin application. **F.** Virus transfected lung cells with 500ng/ml puromycin application.

Photos in Figure 4.8 were taken three days after puromycin selection. Puromycin is a quite effective antibiotic and it is possible to see the effects in three days. However, we could not observe detrimental effects hence; we increased the

concentration of puromycin. For each concentration, we doubled the amount of puromycin meanwhile controls were left unchanged.

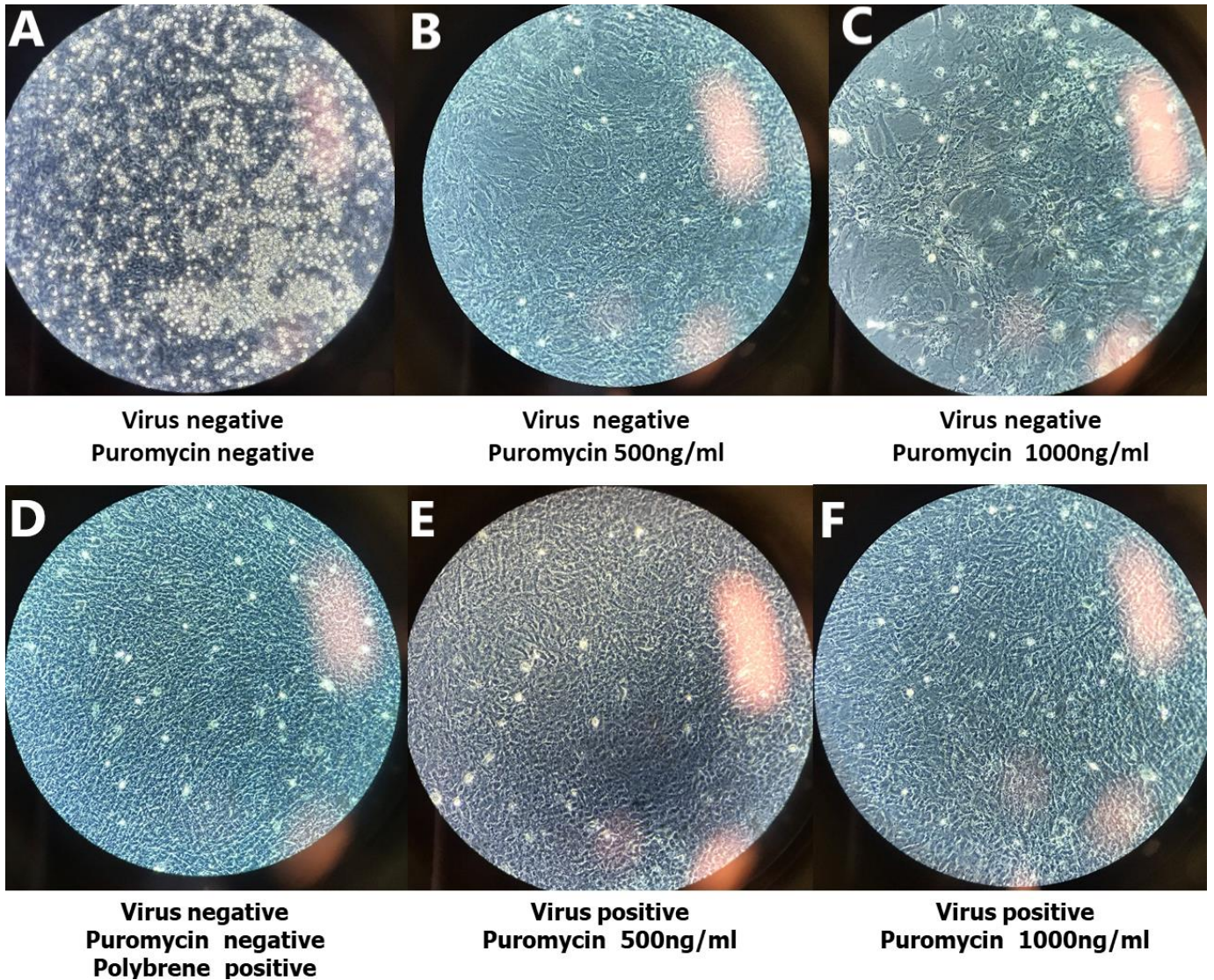


Figure 4.9: Determination of puromycin concentration for selection and control groups. Images were taken under 10x magnification. **A.** Control lung cells without viral transduction and without puromycin application. **B.** Untransduced lung cells with 500ng/ml puromycin application. **C.** Untransduced lung cells with 1000ng/ml puromycin application. **D.** Polybrene control in untransduced and non-puromycin applied cells. **E.** Transduced lung cells with 500ng/ml puromycin application. **F.** Virus transfected lung cells with 1000ng/ml.

Cell photos in Figure 4.9 were taken three days after puromycin application. Although we increased the puromycin concentration twice as high, still we could not observe satisfactory effects even in control groups in Figure 4.9 B and C. We observed cell death in C but not too much and for the virus-transduced cells in E and F, nothing changed in comparison with control groups. This time we increased puromycin concentration to 2000ng/ml and 3000ng/ml.

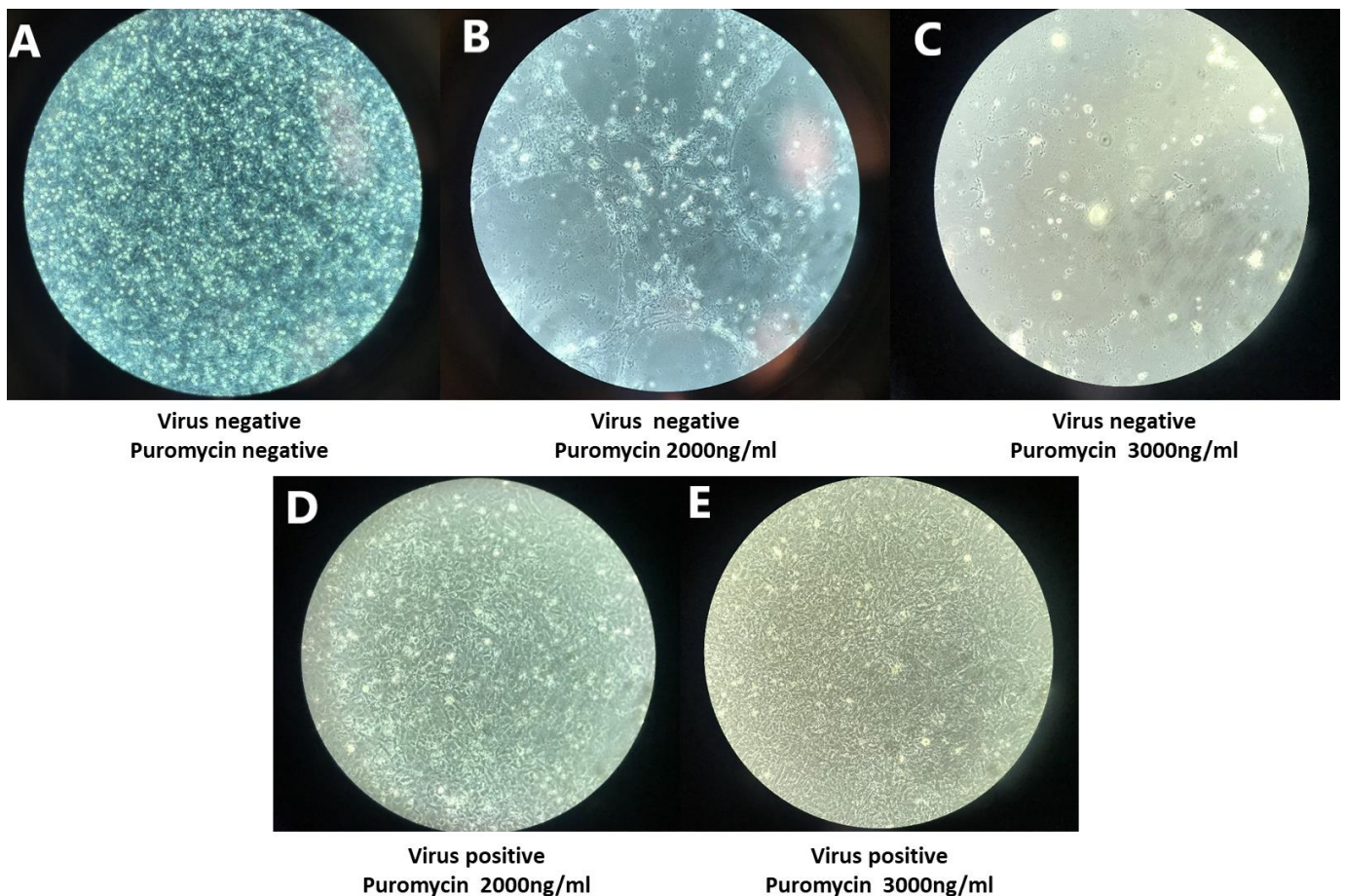


Figure 4.10: Determination of puromycin concentration for selection and control groups. Images were taken under 10x magnification. **A.** Control lung cells without viral transduction and without puromycin application. **B.** Untransduced lung cells with 2000ng/ml puromycin application. **C.** Untransduced lung cells with 3000ng/ml puromycin application. **D.** Transduced lung cells with 200ng/ml puromycin application. **E.** Virus transfected lung cells with 3000ng/ml.

Cell photos in Figure 4.10 were taken four days after 2000ng/ml and 3000ng/ml puromycin applications. Cell deaths were clearly observed in control groups B and C. When we compared the control groups with virus-applied cells, we could say that we selected cells upon puromycin treatment. In order to be sure about our results we waited for two days more and then plated out the cells to transfer into T75 flasks.

We cultured SV40 pBABE puro transduced lung cells allow them to grow. After achieving enough confluency, we decided to do FACS and IF experiments.

4.3 Flow Cytometry and Immunofluorescence Experiments

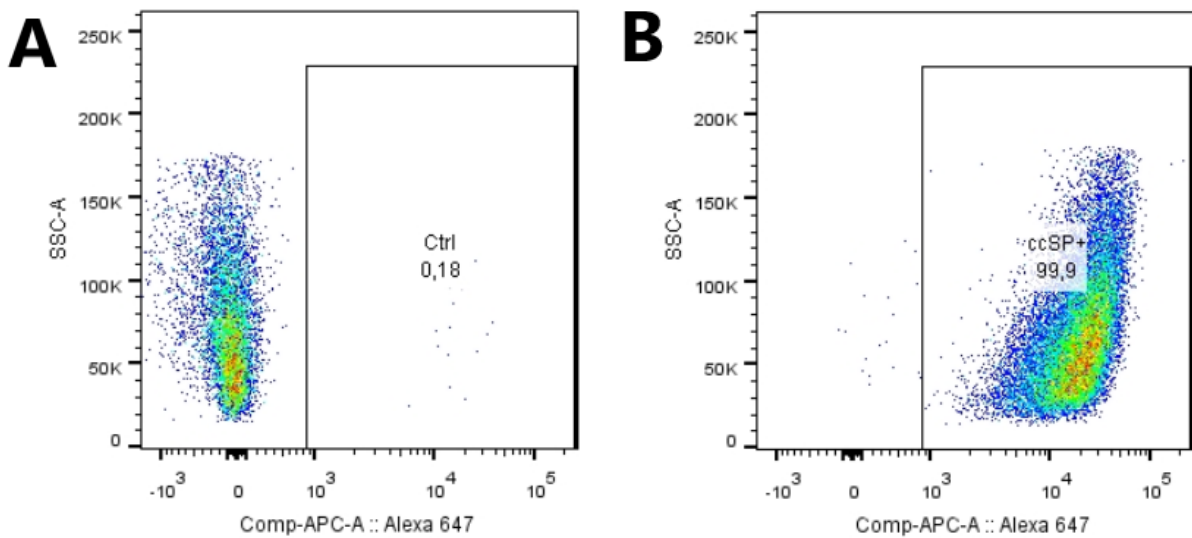


Figure 4.11: Flow cytometry analysis data of transduced cells **A**. Control cells were stained with Alexa Fluor 647. **B**. Immortalized lung cells were fixed and treated with anti-CCSP antibody and then stained with Alexa Fluor 647 for further analysis.

When we obtained enough transfected cells, we performed flow analysis to see if these transfected cells have CCSP+ cell population. Anti-CCSP antibody can be expressed both in the cytoplasm and in the membrane (39). In Figure 4.11, we fixed and permeabilized the cells with CytoFix/CytoPerm buffer (previously explained in Methodology under Intracellular Staining For Flow Cytometry Analysis part). According to flow data, we confirmed that we have CCSP+ cell population so; we decided to proceed with flow cytometry sorting experiment.

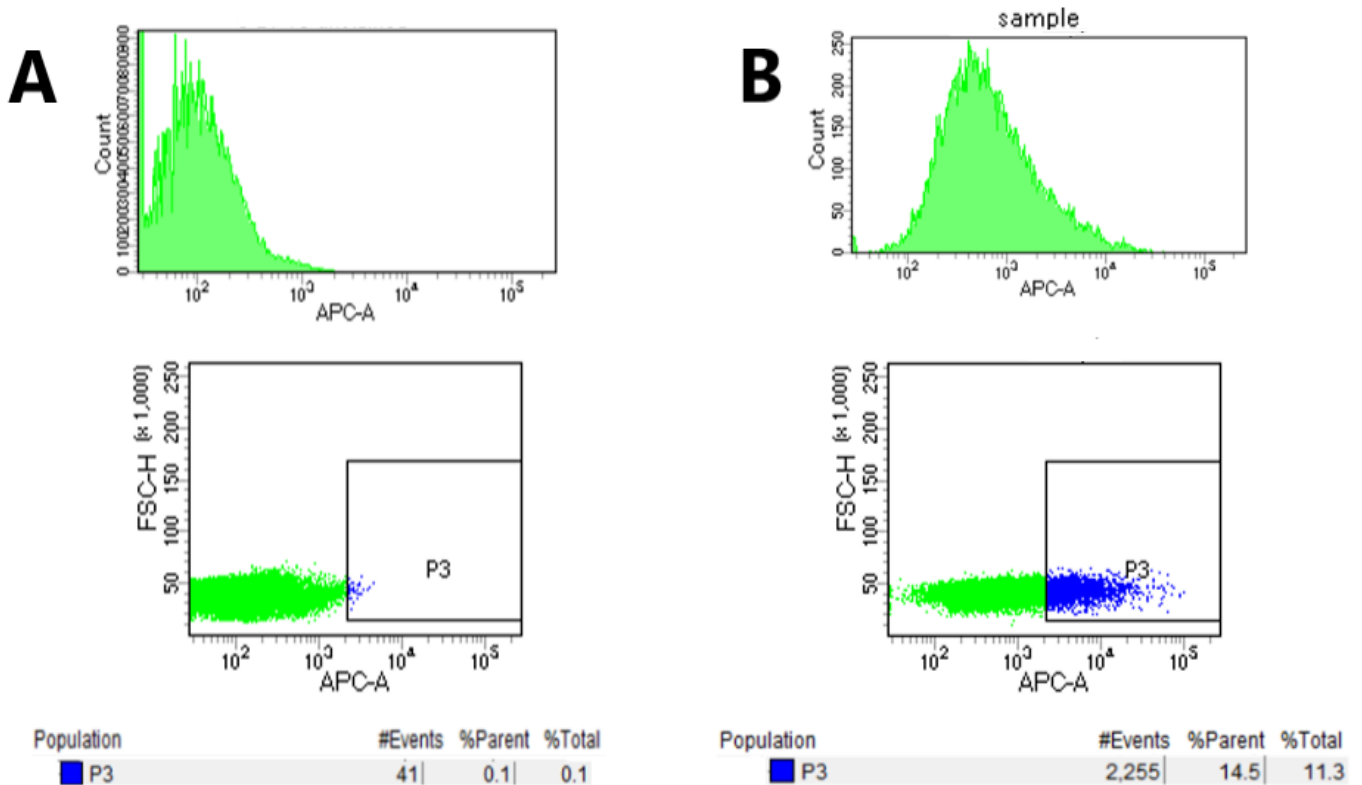


Figure 4.12: FACS ARIA III sorting result. **A.** Cells were stained with with Alexa Fluor 647 secondary antibody. DAPI staining was performed to discriminate dead/alive cells. **B.** CCSP antibody treated cells were stained with Alexa Fluor 647 secondary antibody. DAPI staining was performed to discriminate dead/alive cells. After several gating processes, P3 was chosen as CCSP labeled Alexa Fluor 647⁺ cell population.

In Figure 4.12, transduced lung cells were prepared to select CCSP⁺ cells in crude lung cells. P3 was chosen as CCSP⁺ cell population.

After selection of CCSP⁺ cells, we performed IF experiment to check the purity of these positive cells. Thus, we seeded some cells onto sterilized coverslips placed in 24 well-plate and as a control; we used immortalized unsorted cells (Figure 4.13).

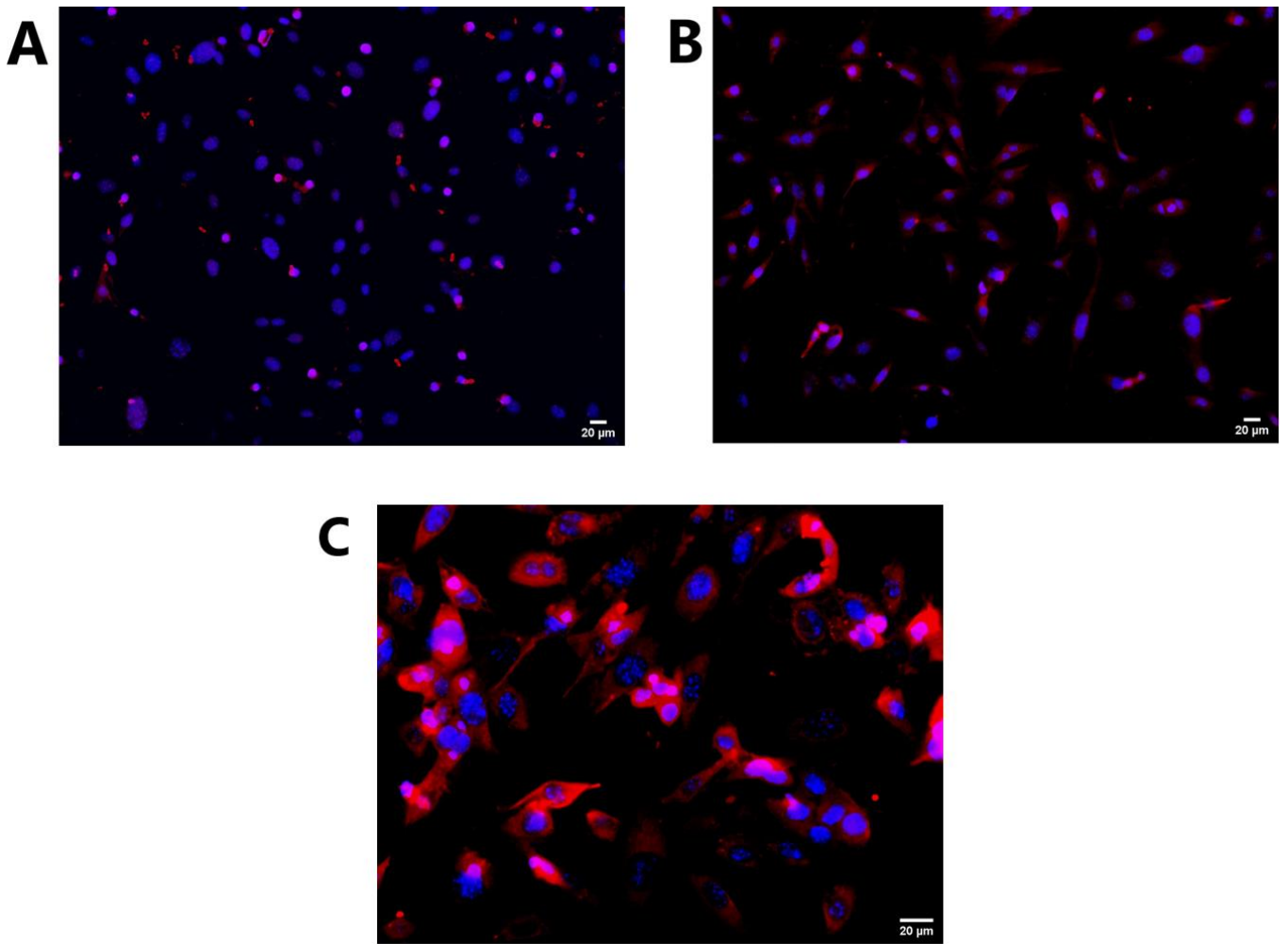


Figure 4.13: Immunofluorescence images CCSP+ cells. **A.** Alexa Fluor 647 staining of unsorted immortalized CCSP labeled lung cells. Images were taken in 20X magnification. **B.** Alexa Fluor 647 staining of sorted immortalized CCSP labeled lung cells. Sorted CCSP+ cells in Figure 4.12 were seeded onto coverslips for IF staining. Images were taken in 20X magnification. **C.** 40x magnified version of cells in B.

We also wanted to check if we have proSPC+ cells in transfected cells. To achieve this, we check transfected cells with flow analysis in terms of proSPC expression. pro-SP-C is found in the cytoplasm (41) so, we performed intracellular staining with the pro-SP-C antibody. Again, cells were fixed and permeabilized then treated with primary and secondary antibodies. In Figure 4.14, flow data confirm that we have also, pro-SP-C+ cells, means we have AECII cell population in our transfected cells.

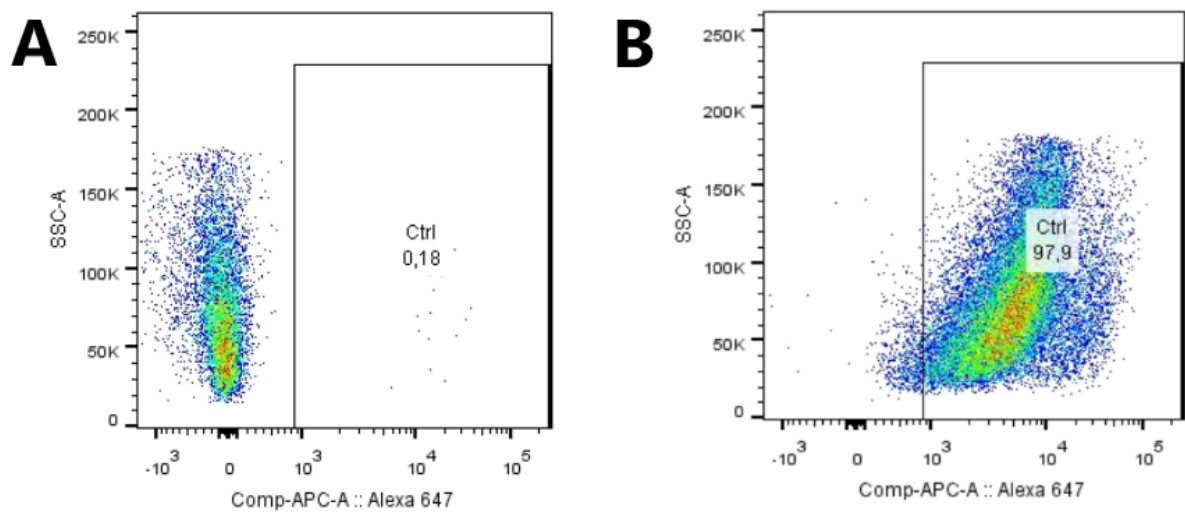


Figure 4.14: Flow cytometry data of proSPC labeled cells. **A.** Control cells were stained with Alexa Fluor 647. **B.** Immortalized lung cells were fixed and intracellular stained. Anti-proSPC antibody was used as primary antibody and then cells were stained with Alexa Fluor 647.

5. DISCUSSION

NSCLC has the highest incidence rate, approximately 80-85%, among all lung cancer types (2). In addition to this, although the five-year survival rate is high in early-stage patients, this rate can fall around 2-3% in patients who diagnosed with advanced-stage NSCLC (3). Detrimental effects of NSCLC are associated with the metastatic capacity of tumor cells. When tumor cells start to spread to other tissues the survival rate directly, decrease in NSCLC.

The cause of low survival rate is, early NSCLC generally remain undiagnosed until disease symptoms occur. Accordingly, a far majority of patients are diagnosed with late stage, metastasizing NSCLC that makes therapeutic intervention rather complicated. Moreover, NSCLC cells either have intrinsic resistance skills or gain resistance to therapies. Under these circumstances, new therapies are required against NSCLC.

During KRAS^{G12D} transformed NSCLC, Alveolar type II and Clara cells were projected as the cell of origin. That is why, in this project, we planned to isolate these cell types and then tried to immortalize them to produce our cell lines. By doing this, we are planning to use them to determine their role during KRAS induced NSCLC in future.

5.1 Acquiring Lung Cells from Mouse Lung Tissue

Genetically modified mice that are planned to be used in this project will come from overseas and this process takes a long time due to international regulations and paper works. When mice arrive, they need extra time to recover before they can be used in experiments. Moreover, they will be grown and mated after their arrival, which will also take time. Therefore, we could not use our mice strains during this project and we used this time interval to optimize the methods.

We used WT C57BL/6 adult mice as a source of lung cells to optimize the cell isolation method. Even working with normal mice, we had many problems during the

procedures. Although, the methods that we refer to are clear, in our case it was not that easy to perform experiments successfully. We had countless complications, had to perform several different experiments, and had to alter materials and methods.

Initially, we used randomly chosen mice with different ages. However, the usage of older than 8 weeks mice caused less cell number release compared to younger mice. Therefore, we decided to use 6-8 weeks old mice.

In the first place, while we were trying to dissociate the lungs, we could not keep lung tissues intact, which causes deficient cell release. Since, during Preparation of the Mouse Lung we did not use catheter so, we could not instill enzyme and agarose properly into lungs that caused deflated lungs rather than enlarged, intact lungs. This instillation problem leads less cell release than expected because the enzyme could not reach to cells deeply. When we achieved to maintain lung tissue integrity and obtained a sufficient amount of cell number, we confronted problems during cell sorting. The viability of sorted cells was too low after sorting.

Primary cells are quite fragile compared to culture cells and the isolation method itself is a stressful procedure for cells, after isolation, performing fluorescence-activated cell sorting causes extra stress on primary cells. That is why we generally obtained less cell numbers than expected. Even when we had enough cells, they could not survive after sorting. Beside isolation and sorting experiments, the health of mice used in experiment may also cause problems. As far as we know, animal facility in IBG have contamination problem and we have learned this problem very recently, during our experiments, acquired cells from contaminated mice might have caused unhealthy cells.

Neither increasing mice number nor improving conditions provided us better yield so, we decided to change our work strategy. According to our initial plan (Figure 3.2) upon acquisition of the interested cell types after isolation, cells would be immortalized by SV40-mediated cell transduction. The aim of the immortalization is to obtain continuously growing cells by disrupting the senescence activity of cells. SV40 Large T antigen directly binds to retinoblastoma (pRB) and tumor suppressor p53 (p53). Large T inactivates pRB and p53 and compels cells to enter S phase (42, 43). Thus, SV40 LT

transfection would provide us with transformed Clara and Alveolar Type II cells. However, we could not obtain enough cells for the immortalization experiment.

Consequently, we changed the workflow to obtain more resistant cells compared to primary cells and performed the immortalization assay before FACS. Nevertheless, there was also a case in which the transfected cells may not be Clara cells or AECII. However, we checked our transfected cells with flow cytometry experiment; in both Figure 4.11 and Figure 4.14 we confirmed that Clara and AECII cells are present in transfected cells. Then we successfully sort Clara cells with ~15% (Figure 4.12).

5.2 Flow Cytometry Experiment

Clara cell sorting is a positive selection by using an anti-CCSP primary antibody and a fluorescently labeled secondary antibody. However, after performing several Clara cell isolation experiments, we had serious shifting problem during sorting. During sorting, fluorescence shifting may occur however; in our case, shifting in x-axis was rapid and happened in a short time period (30 minutes) (Figure 4.4). After reviewing the literature, we found that this problem might due to sample preparation, an improper cell-antibody and/or antibody-antibody interaction, or a FACS Aria III related problem. However, we still do not know why we had this problem since, we prepared the sample as prepared before, we did not change anything during the procedure, we used same antibody in the next experiment. Therefore, we could conclude that maybe the problem was a one-time FACS Aria III-related problem; maybe the machine was contaminated with another analysis before we used the machine. Alternatively, maybe it was due to cell clumping but if this were the case, cells would get stuck in the machine and the machine would give an error since we had clumping problem before and the machine failed. In order to be sure any way we performed following experiments with different secondary antibody, Alexa Fluor 647.

After primary cell immortalization, we performed flow analysis for both Clara cells and AECIIs with their specific antibodies. CCSP antibody can be expressed both in the cytoplasm and in the membrane however, pro-SP-C is an intracellular marker so; we could not use pro-SP-C during sort living cells, unlike CCSP. We prepared the

transfected cells for the analysis and according to our results in Figure 4.11 and Figure 4.14, we can observe both CCSP and pro-SP-C expressions. Although we could see their presence in our immortalized cells, we should have obtained these cells. Thus, we performed sorting experiment for Clara cells. We acquired satisfying CCSP+ cell yield and healthy cells after sorting (Figure 4.12). Further, to validate the purity of these positive cells, some of the sorted cells were seeded onto coverslips for IF experiment and the rest of the cells were cultured. Cultured cells were grown without having detrimental cell loss.

5.3 Immunofluorescence Experiment

In Figure 4.7, we compared normal lung cells with CCSP+ sorted cells. It is possible to see CCSP labeled Alexa Fluor 647 stained cells both in A and B. However, we should have seen CCSP labeled cells more clearly and abundant in B as in Figure 5.1, since after sorting, CCSP cells should have been purified and become distinctive so, Alexa Fluor 647 staining should have been more in B compare to A. Unfortunately in Figure 4.7, CCSP labeled cells are abundant in A compared to B. As expected, we can observe CCSP labeled cells in A and B but we may have lost our CCSP cells during sorting. Although the places of these pictures were randomly selected under the microscope and taken, we had checked all locations under the microscope and still, we had not seen much difference.

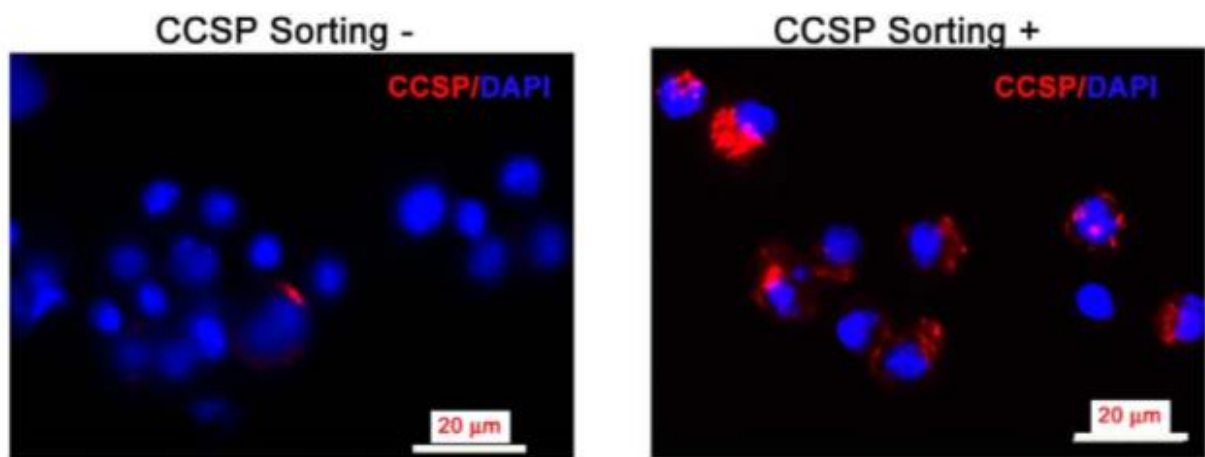


Figure 5.1: Immunofluorescence staining of CCSP labeled cells in Wang, Keefe, Jensen-Taubman, Yang, Yan and Linnoila (39) reference paper. They found that CCSP+ sorted cells were also positive for CCSP IF with higher percentage compared to unsorted cells.

After changing our work plan, and obtaining more resistant cells upon SV40 transfection, we performed another IF staining with sorted cells in order to validate our sorting results in Figure 4.12. In Figure 4.13, IF images of immortalized lung cells were labeled with CCSP and then stained with Alexa Fluor 647. In A, unsorted transfected cells have Alexa Fluor 647 staining that represents CCSP labeled cells but cells in B are more pure and abundant in terms of CCSP labeled cells as expected.

6. CONCLUSIONS AND RECOMMENDATIONS

To conclude, in this project, we achieved to obtain Clara cells from mouse lung tissue. We have transfected cells that we obtained from mouse lung tissue with pBABE SV40 puro plasmid DNA effectively and then select transfected cells upon puromycin application. We were able to maintain these transfected cells in culture environment to allow their growth for several days. Before they started to differentiate, we performed FACS to obtain pure Clara cells and we have successfully sorted these cells.

Although we had unforeseen problems at the beginning of the project, we overcame most of these problems by changing the work plan, methods and materials during the project. However, we failed to complete our hypothesis due to reasons beyond our control. Even though we did not have our mice models to conclude our hypotheses, we have brought the project to a certain point where one can proceed with the project without having any difficulties when mice arrive and are ready for the experiments if they implement the methods exactly as in this project.

In later stages of the project, sorted Clara cells should be sorted for several times until sufficient purity has been reached. The same experiments should also be performed for AECIIs. Moreover, it might also be useful to test these cells with different epithelial markers to ensure that they are the desired cells. For further verification immunofluorescence and western blot experiments might be performed.

7. **REFERENCES**

1. Bray F, Ferlay J, Soerjomataram I, Siegel RL, Torre LA, Jemal A. Global cancer statistics 2018: GLOBOCAN estimates of incidence and mortality worldwide for 36 cancers in 185 countries. *CA Cancer J Clin*. 2018;68(6):394-424. Epub 2018/09/13. doi: 10.3322/caac.21492. PubMed PMID: 30207593.
2. Zappa C, Mousa SA. Non-small cell lung cancer: current treatment and future advances. *Transl Lung Cancer Res*. 2016;5(3):288-300. Epub 2016/07/15. doi: 10.21037/tlcr.2016.06.07. PubMed PMID: 27413711; PMCID: PMC4931124.
3. Lemjabbar-Alaoui H, Hassan OU, Yang YW, Buchanan P. Lung cancer: Biology and treatment options. *Biochim Biophys Acta*. 2015;1856(2):189-210. Epub 2015/08/25. doi: 10.1016/j.bbcan.2015.08.002. PubMed PMID: 26297204; PMCID: PMC4663145.
4. Shanker M, Willcutts D, Roth JA, Ramesh R. Drug resistance in lung cancer. *Lung Cancer (Auckl)*. 2010;1:23-36. PubMed PMID: 28210104.
5. Sutherland KD, Song J-Y, Kwon MC, Proost N, Zevenhoven J, Berns A. Multiple cells-of-origin of mutant K-Ras-induced mouse lung adenocarcinoma. *Proceedings of the National Academy of Sciences*. 2014;111(13):4952-7. doi: 10.1073/pnas.1319963111.
6. Castellano E, Downward J. Role of RAS in the Regulation of PI 3-Kinase. In: Rommel C, Vanhaesebroeck B, Vogt PK, editors. *Phosphoinositide 3-kinase in Health and Disease: Volume 1*. Berlin, Heidelberg: Springer Berlin Heidelberg; 2011. p. 143-69.
7. Meuwissen R, Linn SC, van der Valk M, Mooi WJ, Berns A. Mouse model for lung tumorigenesis through Cre/lox controlled sporadic activation of the K-Ras oncogene. *Oncogene*. 2001;20(45):6551-8. Epub 2001/10/20. doi: 10.1038/sj.onc.1204837. PubMed PMID: 11641780.
8. Jackson EL, Willis N, Mercer K, Bronson RT, Crowley D, Montoya R, Jacks T, Tuveson DA. Analysis of lung tumor initiation and progression using conditional expression of oncogenic K-ras. *Genes Dev*. 2001;15(24):3243-8. Epub 2001/12/26. doi: 10.1101/gad.943001. PubMed PMID: 11751630; PMCID: PMC312845.

9. Hanahan D, Weinberg RA. Hallmarks of cancer: the next generation. *Cell*. 2011;144(5):646-74. Epub 2011/03/08. doi: 10.1016/j.cell.2011.02.013. PubMed PMID: 21376230.
10. Sever R, Brugge JS. Signal transduction in cancer. *Cold Spring Harb Perspect Med*. 2015;5(4). Epub 2015/04/03. doi: 10.1101/cshperspect.a006098. PubMed PMID: 25833940; PMCID: PMC4382731.
11. Herbst RS, Heymach JV, Lippman SM. Lung Cancer. *N Engl J Med*. 2008;359(13):1367-80. doi: 10.1056/NEJMra0802714. PubMed PMID: 18815398.
12. Martin P, Leighl NB, Tsao MS, Shepherd FA. KRAS mutations as prognostic and predictive markers in non-small cell lung cancer. *J Thorac Oncol*. 2013;8(5):530-42. Epub 2013/03/26. doi: 10.1097/JTO.0b013e318283d958. PubMed PMID: 23524403.
13. Vasan N, Boyer JL, Herbst RS. A RAS renaissance: emerging targeted therapies for KRAS-mutated non-small cell lung cancer. *Clin Cancer Res*. 2014;20(15):3921-30. Epub 2014/06/05. doi: 10.1158/1078-0432.CCR-13-1762. PubMed PMID: 24893629; PMCID: PMC5369356.
14. Singh H, Longo DL, Chabner BA. Improving Prospects for Targeting RAS. *J Clin Oncol*. 2015;33(31):3650-9. Epub 2015/09/16. doi: 10.1200/JCO.2015.62.1052. PubMed PMID: 26371146.
15. Drosten M, Dhawahir A, Sum EY, Urosevic J, Lechuga CG, Esteban LM, Castellano E, Guerra C, Santos E, Barbacid M. Genetic analysis of Ras signalling pathways in cell proliferation, migration and survival. *EMBO J*. 2010;29(6):1091-104. Epub 2010/02/13. doi: 10.1038/emboj.2010.7. PubMed PMID: 20150892; PMCID: PMC2845279.
16. Castellano E, Downward J. RAS Interaction with PI3K: More Than Just Another Effector Pathway. *Genes Cancer*. 2011;2(3):261-74. doi: 10.1177/1947601911408079. PubMed PMID: 21779497.
17. Gysin S, Salt M, Young A, McCormick F. Therapeutic strategies for targeting ras proteins. *Genes Cancer*. 2011;2(3):359-72. Epub 2011/07/23. doi: 10.1177/1947601911412376. PubMed PMID: 21779505; PMCID: PMC3128641.

18. Bhattacharya S, Socinski MA, Burns TF. KRAS mutant lung cancer: progress thus far on an elusive therapeutic target. *Clin Transl Med.* 2015;4(1):35. Epub 2015/12/17. doi: 10.1186/s40169-015-0075-0. PubMed PMID: 26668062; PMCID: PMC4678136.
19. O'Hagan RC, Heyer J. KRAS Mouse Models: Modeling Cancer Harboring KRAS Mutations. *Genes Cancer.* 2011;2(3):335-43. Epub 2011/07/23. doi: 10.1177/1947601911408080. PubMed PMID: 21779503; PMCID: PMC3128636.
20. DuPage M, Dooley AL, Jacks T. Conditional mouse lung cancer models using adenoviral or lentiviral delivery of Cre recombinase. *Nat Protoc.* 2009;4(7):1064-72. Epub 2009/06/30. doi: 10.1038/nprot.2009.95. PubMed PMID: 19561589; PMCID: PMC2757265.
21. Rowbotham SP, Kim CF. Diverse cells at the origin of lung adenocarcinoma. *Proceedings of the National Academy of Sciences.* 2014;111(13):4745-6. doi: 10.1073/pnas.1401955111.
22. Boers JE, Ambergen AW, Thunnissen FB. Number and proliferation of clara cells in normal human airway epithelium. *Am J Respir Crit Care Med.* 1999;159(5 Pt 1):1585-91. Epub 1999/05/06. doi: 10.1164/ajrccm.159.5.9806044. PubMed PMID: 10228131.
23. Rokicki W, Rokicki M, Wojtacha J, Dzelijli A. The role and importance of club cells (Clara cells) in the pathogenesis of some respiratory diseases. *Kardiochir Torakochirurgia Pol.* 2016;13(1):26-30. Epub 2016/05/24. doi: 10.5114/kitp.2016.58961. PubMed PMID: 27212975; PMCID: PMC4860431.
24. Atkinson JJ, Adair-Kirk TL, Kelley DG, Demello D, Senior RM. Clara cell adhesion and migration to extracellular matrix. *Respir Res.* 2008;9:1. Epub 2008/01/09. doi: 10.1186/1465-9921-9-1. PubMed PMID: 18179694; PMCID: PMC2249579.
25. Feher J. The Mechanics of Breathing. *Quantitative Human Physiology* 2017. p. 623-32.
26. Kim HJ, Ingbar DH, Henke CA. Integrin mediation of type II cell adherence to provisional matrix proteins. *American Journal of Physiology-Lung Cellular and*

- Molecular Physiology. 1996;271(2):L277-L86. doi: 10.1152/ajplung.1996.271.2.L277. PubMed PMID: 8770067.
27. MASON RJ. Biology of alveolar type II cells. *Respirology*. 2006;11(s1):S12-S5. doi: 10.1111/j.1440-1843.2006.00800.x.
 28. Li F, He J, Wei J, Cho WC, Liu X. Diversity of epithelial stem cell types in adult lung. *Stem Cells Int*. 2015;2015:728307. Epub 2015/03/27. doi: 10.1155/2015/728307. PubMed PMID: 25810726; PMCID: PMC4354973.
 29. Walker C, Mojares E, Del Rio Hernandez A. Role of Extracellular Matrix in Development and Cancer Progression. *Int J Mol Sci*. 2018;19(10). Epub 2018/10/06. doi: 10.3390/ijms19103028. PubMed PMID: 30287763; PMCID: PMC6213383.
 30. Stupack DG. Get a ligand, get a life: integrins, signaling and cell survival. *J Cell Sci*. 2002;115(19):3729-38. doi: 10.1242/jcs.00071.
 31. Longmate W, DiPersio CM. Beyond adhesion: emerging roles for integrins in control of the tumor microenvironment. *F1000Research*. 2017;6:1612. Epub 2017/10/14. doi: 10.12688/f1000research.11877.1. PubMed PMID: 29026524; PMCID: PMC5583736.
 32. Hamidi H, Pietilä M, Ivaska J. The complexity of integrins in cancer and new scopes for therapeutic targeting. *Br J Cancer*. 2016;115(9):1017-23. Epub 2016/09/29. doi: 10.1038/bjc.2016.312. PubMed PMID: 27685444.
 33. Hamidi H, Ivaska J. Every step of the way: integrins in cancer progression and metastasis. *Nat Rev Cancer*. 2018;18(9):533-48. Epub 2018/07/14. doi: 10.1038/s41568-018-0038-z. PubMed PMID: 30002479.
 34. Sulzmaier FJ, Jean C, Schlaepfer DD. FAK in cancer: mechanistic findings and clinical applications. *Nature Reviews Cancer*. 2014;14:598. doi: 10.1038/nrc3792.
 35. Carelli S, Zadra G, Vaira V, Falleni M, Bottiglieri L, Nosotti M, Di Giulio AM, Gorio A, Bosari S. Up-regulation of focal adhesion kinase in non-small cell lung cancer. *Lung Cancer*. 2006;53(3):263-71. doi: 10.1016/j.lungcan.2006.06.001.
 36. Peng J, Gassama-Diagne A. Apicobasal polarity and Ras/Raf/MEK/ERK signalling in cancer. *Gut*. 2017;66(6):986-7. Epub 2016/12/16. doi: 10.1136/gutjnl-2016-312986. PubMed PMID: 27974551.

37. Mummery C. Harnessing the power of cardiac stem cells. *Cell and Gene Therapy Insights*. 2016;2(3):391-6. doi: 10.18609/cgti.2016.041.
38. Frappart DdS, Maurisse R, Vock EH, Gruenert DC. Immortalization Strategies for Epithelial Cells in Primary Culture. *Drug Absorption Studies*2008. p. 616-39.
39. Wang XY, Keefe KM, Jensen-Taubman SM, Yang D, Yan K, Linnoila RI. Novel method for isolation of murine clara cell secretory protein-expressing cells with traces of stemness. *PLoS One*. 2012;7(8):e43008. Epub 2012/08/24. doi: 10.1371/journal.pone.0043008. PubMed PMID: 22916196; PMCID: PMC3420884.
40. Gereke M, Autengruber A, Grobe L, Jeron A, Bruder D, Stegemann-Koniszewski S. Flow cytometric isolation of primary murine type II alveolar epithelial cells for functional and molecular studies. *J Vis Exp*. 2012(70). Epub 2013/01/05. doi: 10.3791/4322. PubMed PMID: 23287741; PMCID: PMC3576420.
41. Sinha M, Lowell CA. Isolation of Highly Pure Primary Mouse Alveolar Epithelial Type II Cells by Flow Cytometric Cell Sorting. *Bio Protoc*. 2016;6(22). Epub 2017/02/10. doi: 10.21769/BioProtoc.2013. PubMed PMID: 28180137; PMCID: PMC5293249.
42. Ryu W-S. Tumor Viruses. *Molecular Virology of Human Pathogenic Viruses*2017. p. 335-49.
43. Ahuja D, Saenz-Robles MT, Pipas JM. SV40 large T antigen targets multiple cellular pathways to elicit cellular transformation. *Oncogene*. 2005;24(52):7729-45. Epub 2005/11/22. doi: 10.1038/sj.onc.1209046. PubMed PMID: 16299533.